PERMEABILITY OF MUSCLE CAPILLARIES TO EXOGENOUS MYOGLOBIN

NICOLAE SIMIONESCU, MAIA SIMIONESCU, and GEORGE E. PALADE

From The Rockefeller University, New York 10021. Doctors Simionescu's permanent address is the Institute of Endocrinology, Bucharest, Romania.

ABSTRACT

Whale skeletal muscle myoglobin (mol wt 17,800; molecular dimensions 25 × 34 × 42 Å) was used as a probe molecule for the pore systems of muscle capillaries. Diaphragms of Wistar-Furth rats were fixed *in situ* at intervals up to 4 h after the intravenous injection of the tracer, and myoglobin was localized in the tissue by a peroxidase reaction. Gel filtration of plasma samples proved that myoglobin molecules remained in circulation in native monomeric form. At 30–35 s postinjection, the tracer marked ~75% of the plasmalemmal vesicles on the blood front of the endothelium, 15% of those located inside and none of those on the tissue front. At 45 s, the labeling of vesicles in the inner group reached 60% but remained nil for those on the tissue front. Marked vesicles appeared on the latter past 45 s and their frequency increased to ~80% by 60–75 s, concomitantly with the appearance of myoglobin in the pericapillary spaces. Significant regional heterogeneity in initial labeling was found in the different segments of the endothelium (i.e., perinuclear cytoplasm, organelle region, cell periphery, and parajunctional zone). Up to 60 s, the intercellular junctions and spaces of the endothelium were free of myoglobin reaction product; thereafter, the latter was detected in the distal part of the intercellular spaces in concentration generally equal to or lower than that prevailing in the adjacent pericapillary space. The findings indicate that myoglobin molecules cross the endothelium of muscle capillaries primarily via plasmalemmal vesicles. Since a molecule of this size is supposed to exit through both pore systems, our results confirm the earlier conclusion that the plasmalemmal vesicles represent the large pore system; in addition, they suggest that the same structures are, at least in part, the structural equivalent of the small pore system of this type of capillaries.

INTRODUCTION

The plasmalemmal vesicles of the endothelium have been identified as the structural equivalent of the large pore system in the blood capillaries of skeletal muscle (rat diaphragm) by using ferritin (molecular diameter [md][1] ≃ 110 Å) as a particulate tracer (1), but the structural identity of the small pore system in the same type of vessels is still in doubt. Using horseradish peroxidase (HRP) (mol wt ≃ 40,000, md ≃ 40–50 Å) as a histochemically detectable tracer, Karnovsky (2) and Cotran and Karnovsky (3) arrived at the conclusion that it reaches the pericapillary spaces mainly through the intercellular junctions of the

[1] *Abbreviations used in this paper*: d, diameter; HRP, horse radish peroxidase; i.v., intravenous; Mb, myoglobin; md, molecular diameter.

endothelium, and identified these junctions as a slit variety of small pores. Other investigators found, however, that the HRP reaction product does not penetrate the intercellular spaces of the endothelium beyond lines tentatively identified as tight junctions in the capillaries of skeletal muscle (4) and myocardium (5). Moreover, the results obtained with HRP appear to depend on dose (6), injected volume (7), and osmolarity of the tracer solution (8). On account of its relatively large dimensions, HRP is considered at present as a probe of marginal value for the small pore system, and the need for smaller tracers is generally recognized. Karnovsky has published preliminary findings (9) obtained with cytochrome *c* (mol wt 12,000; mds $\sim 30 \times 34 \times 34$ Å [10]) which, in his interpretation, support the conclusions of his work with HRP, but the usefulness of this tracer is limited by difficulties encountered in its histochemical detection.

In this article we report results obtained with myoglobin (Mb) which, as a probe, has the following advantages: (*a*) it is a globular, compact molecule with a well-established tertiary structure (11, 12); (*b*) it is smaller than HRP (mol wt 17,800; mds $25 \times 34 \times 42$ Å or 33 $Å_{avg}$ [11, 12]); (*c*) it gives stable monomer solutions over a wide range of concentrations,[2] pHs,[3] and temperatures[4] (13–25, 27–29), and (*d*) it has detectable peroxidatic activity which has already been used for the localization of endogenous Mb (30–33).

[2] The compact structure of Mb in crystals as well as in solution (13–15) is thermodynamically stable over a relatively large range of concentrations. Up to a concentration of 10% (w/v), the diffusion coefficient is concentration independent (16); close packing occurs only at concentrations of 48% with the molecules still undergoing translational movements at a high rate (16).

[3] The oxygen affinity of Mb is essentially pH independent (17) and alkylation does not alter the properties of the molecules in the pH range 8–10 (18). The alkylated molecules are more stable against heat (19–21) or acetone extraction (22). At pH 4.0–4.5 small amounts of heme are extracted, and at pH 3.2–2.2 the molecule is finally fully denatured (20).

[4] The spectrum of Mb solutions is stable over the temperature range 7.5 to 37°C (18, 20, 23–26); changes occur only above 40°C temperature at which the molecules eventually polymerize and precipitate (27). The Mb molecule has no sulfhydryl and disulfide groups (27, 28), which can explain the absence of molecular interactions and polymerization.

MATERIALS AND METHODS

Materials

Mb SOURCES: Saltfree, crystallized Mbs 95–100% pure were obtained from the following sources: (*a*) *Whale skeletal muscle Mb* (Type II, Fe-content ~0.30%, primarily in the ferric form) from Sigma Chemical Co., St. Louis, Mo; Nutritional Biochemical Corp., Cleveland, Ohio; Schwarz/Mann Div., Becton, Dickinson and Co. Orangeburg, N.Y.; and Miles Laboratories, Miles Research Div., Kankakee, Ill. (*b*) *Equine skeletal muscle Mb* (Type I, Fe-content ~0.30%) from Sigma Chemical Co., and Miles Laboratories. (*c*) *Horse heart Mb* from Nutritional Biochemical Corp., and Schwarz/Mann Div.

All preparations were well tolerated in intravenous (i.v.) injections and all gave a detectable peroxidase reaction in the plasma. The best results, in terms of density and homogeneity of the reaction product, were obtained with whale skeletal muscle Mb (Sigma Chemical Co.). The observations here reported were made exclusively with this Mb.

PREPARATION OF TRACER SOLUTIONS: Mb crystals were dissolved in 0.154 M NaCl at concentrations usually ranging from 1 to 5% and the pH of the solutions was adjusted to 7.0–7.6 with 0.1 N NaOH. Before use, the solutions were sonicated for 10 min at ~22°C at 40 mA in an ultrasonic tank (Dr 50 H, Acoustica Associates, Inc., Van Nuys, Calif.) and in some cases their temperature was brought up to 38°C. Over the concentration, pH, and temperature range mentioned, the solutions showed a homogeneous, monomeric dispersion (see Results) and gave an intense peroxidatic reaction.

ANIMALS: The experiments were carried out on rats of the Wistar-Furth strain (Microbiological Associates, Inc., Bethesda, Md.), known to be genetically resistant to histamine release by dextrans (34, 35), Glycogens (35), and HRP (36). Our experiments show that the same applies to exogenous Mb. We used 108 male, young adults (100–135 g) for the Mb experiments and 46 for different controls (Table I). All animals were kept under standardized housing and feeding conditions for a few days before use.

Methods

CONTROL FOR VASCULAR LEAKAGE

Vascular leakage was checked by previously published procedures (35, 37). Mb solution (0.05 ml of 1% Mb solution), prepared as given above, was injected under the skin of the anterior face of the scrotum. The hypodermis and the subjacent cremaster were examined 1 h later for signs of the vascular "tattoo" that accompanies plasma leakage (35, 37).

Tracer Injection

Mb solutions were injected under ether anesthesia (38) in the saphenous vein over an interval of 5–10 s, the volume injected being adjusted to 10% of the estimated total blood volume (39). With this amount, and at the concentrations used in most experiments (1–2%), the exogenous Mb is expected to increase transiently the osmotic pressure of the plasma by 4–8%. In some experiments higher Mb concentrations (up to 20%) were used; no difference in results was recorded between low and high concentrations.

Tissue Processing

FIXATION: Of the fixatives (e.g., acrolein, formaldehyde, glutaraldehyde, and mixtures of the last two) and buffers (HCl-Na cacodylate, K-phosphates, Na arsenate [H_3AsO_4-Na_2HAsO_4]) tested, the best results were obtained with a mixture of 5% formaldehyde, and 3% glutaraldehyde in 0.1 M Na arsenate buffer pH 7.1–7.4. The mixture was warmed up to 38°C and injected under anesthesia in the pleural and peritoneal cavities. Fixation was started either simultaneously with the Mb injection or at chosen intervals from 5 s to 4 h after it (Table I). After 10 min fixation *in situ*, the diaphragm was excised and cut into small strips (0.5–1 mm) which were immersed in the same fixative for 90 min at room temperature, and finally washed in 0.1 M Na arsenate buffer (20 min).

Acrolein was tried because of its rapid diffusion and fast action, but was found unsatisfactory since it did not fully retain the luminal plasma and partially inactivated the Mb. Fixation in arsenate buffer gave better preservation and higher contrast of endothelial details than fixation in the other buffers mentioned.

CYTOCHEMICAL REACTION—POSTFIXATION: The fixed and washed tissue was cut on a Smith-Farquhar TC2 tissue chopper (Ivan Sorvall, Inc. Newtown, Conn.) into 40–50-μm thick slices which were incubated in a Graham-Karnovsky mixture (40), modified for optimal results with Mb (0.15% 3,3′-diaminobenzidine tetrachloride and 0.02% H_2O_2 in 0.06 M HCl-Tris buffer, pH 8.0–8.2). The reaction was carried out at room temperature for 60 min and was terminated by washing the specimens in distilled water (10 min) and transferring them to 2% OsO_4 in 0.05 M Na arsenate buffer, pH 7.1–7.2, for 90 min at room temperature for postfixation.

STAINING IN BLOCK: None of the procedures used, i.e. ferricyanide during postfixation (41) and uranyl acetate (42) or uranyl oxalate-acetate (43) before dehydration, gave useful results since they caused an uneven increase in the density of the ground substance in the pericapillary spaces which proved to be high enough to interfere with the reliable visualization of the reaction product.

DEHYDRATION, EMBEDDING: Without washing, the postfixed tissues were rapidly (25 min) dehydrated in 95 and 100% ethanol at 4°C, and finally embedded in Epon in flat molds (44).

SECTIONING: Sections were cut at 100–200 nm for general survey in the light microscope, and at ~60 nm for electron microscopy on an MT 2B Porter-Blum ultramicrotome (Ivan Sorvall, Inc.), fitted with diamond knives. To facilitate detection of the reaction product, especially when in low concentration, the sections were examined either unstained or lightly stained (0.5–2 min) in lead citrate.

MICROSCOPY: We used either a Philips 300 or a Siemens-Elmiskop I electron microscope, operated at 80 kV and provided with a 200 μm condensor aperture and a 30 μm objective aperture. The instruments were calibrated with a cross-lined carbon grating replica having 2160 lines/mm.

QUANTITATIVE MEASUREMENTS: For estimating the aggregated volume occupied by different

TABLE I

Time Intervals and Number of Animals Used in Myoglobin Experiments

(For each animal, four to five samples of diaphragm were examined by electron microscopy.)

	Intervals*									Total no. of rats (122)§
	Phase I 30‡–35 s	Phase II 35–45 s	Phase III 45–60 s	Phase IV 60–75 s	1.5–5 min	10–15 min	30 min	1–2 h	4 h	
Mb injected	18	19	14	16	13	12	6	5	5	108
Controls (non-injected)										14

* Time points were counted from the beginning of the injection and include additional 30 s as average estimated period for the local blood flow arrest by the fixation *in situ* (see Methods).

‡ The intravenous Mb injection and the fixation *in situ* were performed in the same time.

§ In addition to that, 32 rats were used for control experiments (red blood cell hemolysis, arrest of blood flow by fixative, test for vascular leakage, etc.).

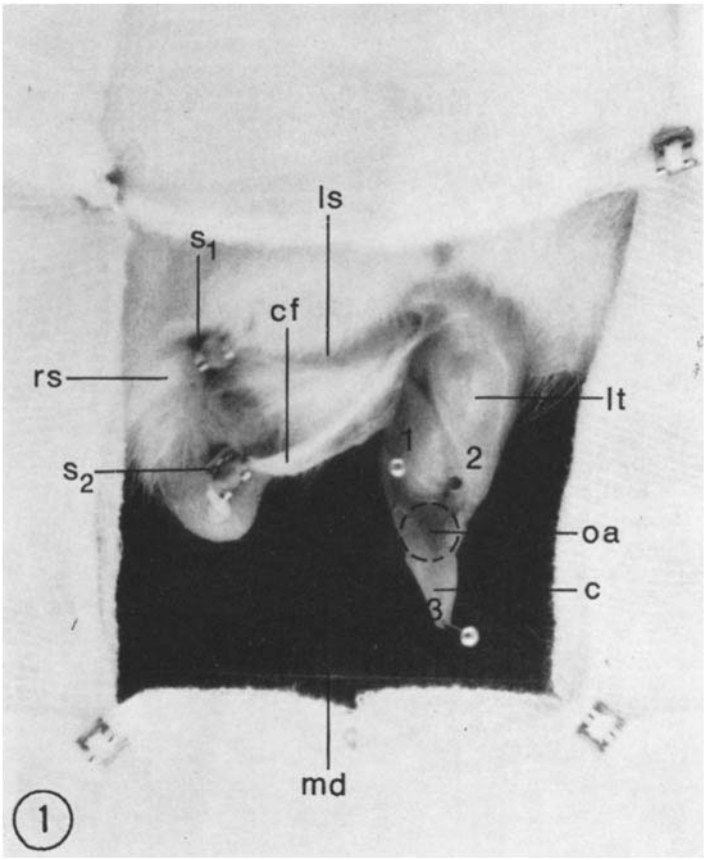

General abbreviations used in legends:

bm, basement membrane
c, collagen fibers
cv, chain of plasmalemmal vesicles
e, endothelium
ec, erythrocyte
er, endoplasmic reticulum
f, fibroblast
g, Golgi apparatus
j, intercellular junction
i, intercellular space
l, capillary lumen
m, muscle cell
mc, macrophage
md, mitochondria
n, nucleus
or, organelle region
p, pericyte
pc, cell periphery zone
pj, parajunctional zone
pn, perinuclear cytoplasm
pp, pericyte pseudopodia
ps, pericapillary space
sv, sarcolemmal vesicle
v, plasmalemmal vesicle
vb, plasmalemmal vesicle (blood front)
vi, plasmalemmal vesicle (inside the cytoplasm)
vt, plasmalemmal vesicle (tissue front)

Figs. 9, 11, 12, 13, 20, 21 *a*, 25 *b*, and 26 represent unstained sections; the others were stained for 1–3 min only in lead citrate.

FIGURE 1 Operative preparation for checking the time required by the fixative to arrest cremasteric blood flow. Ventral view. The cut skin of left scrotum (*ls*) is fixed by a staple (S_1) to the opposite scrotum (*rs*); the dissected and partially removed cremasteric facia (*cf*) is also fixed to the opposite scrotum by another staple (S_2); the left testicle (*lt*) is pushed up by two needles (1 and 2) piercing the mincing dish (*md*) used as support, while a third needle (3) fixes the gently stretched cremaster muscle (*c*); the observation area (*oa*) is illuminated and brought under the microscope objective. × 1.5.

segments of the endothelium, measurements were carried out on electron micrographs with a calibrated × 7 magnifier and a Keuffel and Esser planimeter (Keuffel and Esser Co., Morristown, N.J.).

Tracer Controls

The following procedures were used to check the purity of the Mb solutions to be injected and the size and state of dispersion of the Mb molecules in these solutions and in the blood plasma.

GEL CHROMATOGRAPHY: Gel filtration was performed on 1 × 90 cm Sephadex G-75 columns (Pharmacia Fine Chemicals Inc., Uppsala, Sweden) equilibrated with 0.1 M NH_4HCO_3 buffer, pH 8.0. Elution was carried out with the same buffer at a flow rate of 6 ml/h. Protein concentration in the eluate was continuously recorded as transmission at 280 nm with a Uvicord II ultraviolet absorptiometer (LKB Produkter, Stockholm, Sweden). In the graphs, the data are plotted as absorbancy at 280 nm. The effluent was finally collected in 3 ml fractions using an ISCO fraction collector (Instrumentation Specialties Co., Lincoln, Neb.).

SPECTROPHOTOMETRY: The absorbance of the fractions collected as above was measured at 415 nm (maximum for ferrihemoproteins, including ferrimyoglobin [45, 46]) with a Zeiss PMQ II spectrofluorometer (Carl Zeiss, Inc., New York). The readings were taken at 25°C in 1 mm cells against a reagent blank (0.1 M NH_4HCO_3).

NEGATIVE STAINING: Samples of Mb solution, blood plasma collected from injected animals, and serum-Mb mixtures (prepared in vitro) were examined by negative staining using 0.5% uranyl oxalate adjusted to pH 7.0 (47). The procedure is known to give reliable results with small proteins (48, 49), including cytochrome *c* (50), hemoglobin subunits, and Mg (51).

CONTROL FOR FIXATIVE-INDUCED HEMOLYSIS: Since aldehyde fixation has been reported to induce hemolysis (52) and since leaking hemoglobin can impart a positive peroxidatic reaction to the plasma, we ran controls on diaphragm samples collected from noninjected rats, and fixed, reacted for peroxidase activity, and processed as given under tissue processing.

Time Required for the Arrest of Blood Flow by the Fixative

Since the capillaries of the diaphragm cannot be directly examined in vivo, we used a cremaster preparation, described in detail in the legend of Fig. 1, to measure the lag between the beginning of fixation *in situ* and the arrest of the local blood circulation. The chosen area was examined under a dissecting microscope at × 85 magnification, using a combination of epi- and transillumination. The fixative was injected into the *tunica vaginalis* and at the same time pipetted on the cremaster under visual (microscopic) control, and the time was counted until blood flow stopped in the local vascular bed. This procedure is simpler than those already recorded in the literature (53–57); in addition it minimizes the traumatism and avoids the incision of the cremaster.

RESULTS

State of Mb

A first series of experiments was carried out to determine the state of Mb in the tracer solution and in the blood plasma over the period pertinent to our observations.

IN THE TRACER SOLUTION: Gel chromatography of samples of the solution to be injected showed that Mb elutes essentially as a single, symmetric peak at the expected position of the monomer with only 4–5% of the molecules behaving as small aggregates (Fig. 2). The material under the monomer peak was further characterized by spectrophotometry which showed that it absorbs intensely at 415 nm (the Soret band of Mb). Finally, in negatively stained samples of the Mb solution we found that $\gtrsim$90% of the molecules had the spherical or ovoid shape and the dimensions expected for the monomer (Fig. 3). About 70% of the molecules measured 30–40 Å; ~24% were in the range 40–50 Å, and only a few appeared larger (70–100 Å) (Fig. 4). The first two groups are assumed to represent different orientations of the molecules in respect to the supporting film; the last group is made up by aggregates. The results obtained by electron microscopy are in

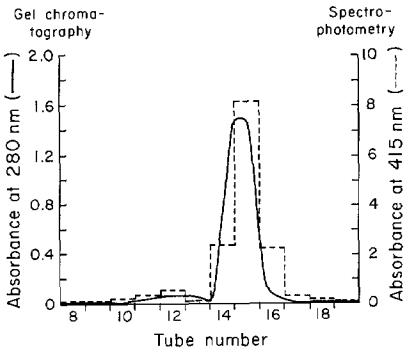

FIGURE 2 Gel chromatography (Sephadex G-75) and spectrophotometry (at 415 nm) of a 15% Mb solution in isotonic saline at pH 7.0. A sample of this solution used for negative staining is shown in Fig. 3.

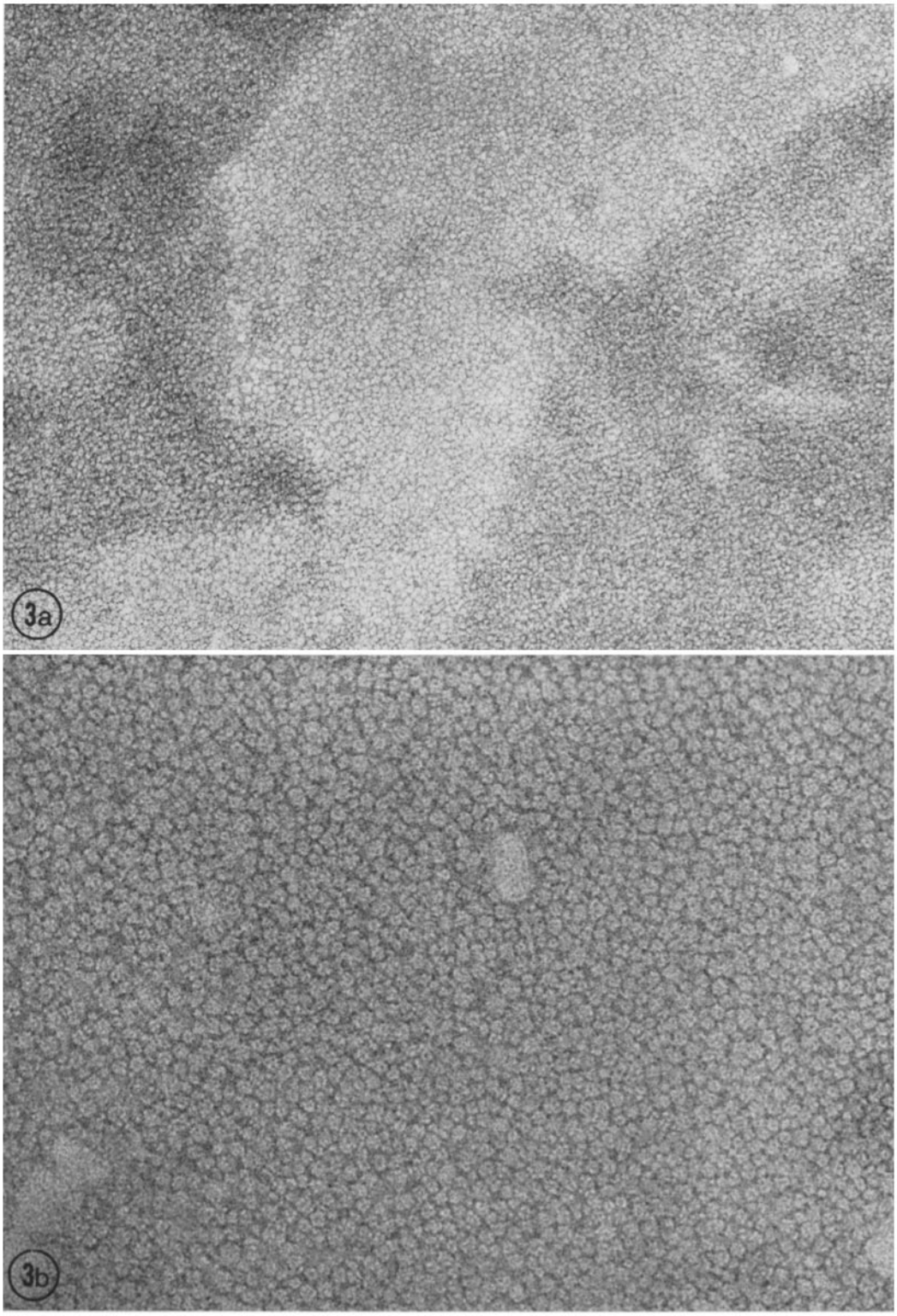

FIGURES 3 *a, b* Negatively stained Mb molecules (0.5% uranyl acetate oxalate, pH 7.0) in samples of solutions prepared for intravenous injection. (*a*) × 210,000; (*b*) × 650,000.

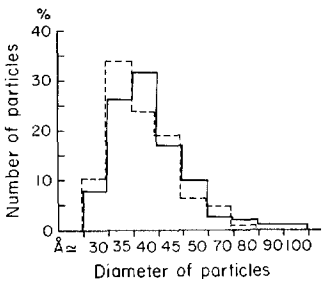

FIGURE 4 Size distribution of Mb molecules in solutions prepared for intravenous injection (——), and in the blood plasma, 10 min after injection (----). For these determinations, 2,400 and 1,800 molecules, respectively, were measured on micrographs of negatively stained preparations.

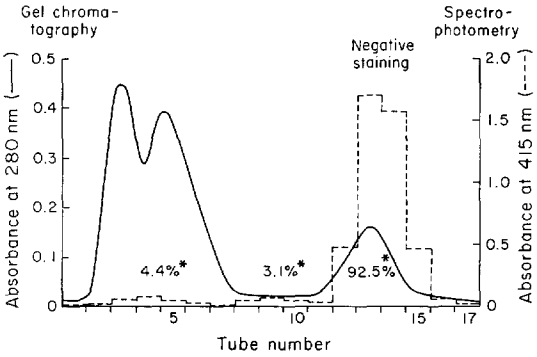

FIGURE 5 Gel chromatography (Sephadex G-75) and spectrophotometry (at 415 nm) of a serum sample (0.2 ml) collected 10 min after injecting intravenously 1 ml/100 g body weight of 5% Mb solution in a rat with ligatured renal vessels. A sample from tube no. 13 was negatively stained (see Fig. 7). The material absorbing at 415 nm is Mb in fractions 12–15, Mb aggregates in fractions 8–10, and probably hemoglobin in fractions 2–5. * The figures represent percentages from the total amount of material absorbing at 415 nm.

good agreement with data obtained by X-ray diffraction.

IN THE CIRCULATING PLASMA: Gel chromatography of plasma samples collected from animals 10 min after a Mb injection showed that the tracer is present in monomeric form, as indicated by the position of the peak (Fig. 5) and by the electron microscopy of negatively stained samples (Fig. 6) taken therefrom. There was no evidence of Mb adsorption to plasma proteins. Spectrophotometry of the eluted fractions confirmed these results and revealed, in addition, the presence of a small flat peak of OD_{421} in the region of plasma proteins (Fig. 5).

Similar results were obtained with an in vitro mixture of serum and Mb solution (Fig. 7).

The small flat OD_{415} peak under the plasma proteins is probably due to a limited amount of hemoglobin released during the preparation of the specimens. A similar peak was detected in the serum of control animals, in the absence of Mb injection.

Other Sources of Peroxidatic Activity

Other experiments were done to find out whether any peroxidatic activity can be detected in the plasma in the absence of injected Mb. Such an activity could be due to hemoglobin diffusing out of erythrocytes, partially plasmolyzed during aldehyde fixation (52). The examination of diaphragm specimens collected from rats not injected with Mb showed no peroxidase reaction in the plasma in sections of blood capillaries which contained no erythrocytes in their lumina. But a faint reaction was detected in association with intraluminal erythrocytes; it was limited in extent (50–100 nm), usually one-sided, probably reflecting the main direction of diffusion of the fixative, and weak enough not to interfere with our observations. In any case we decided to compare systematically capillaries with and without erythrocytes in our Mb experiments.

A low OD_{415} peak, presumably due to hemoproteins, is found under the plasma protein peak in the chromatograms of plasma collected from Mb-injected rats, as well as in mixtures of normal serum and Mb solutions. The peak could represent free hemoglobin or Mb aggregates. The former interpretation is favored, since a similar peak is found in the serum of normal rats not injected with Mb and its size can be increased by manipulations which traumatize the erythrocytes.

Vascular Leakage

Finally we checked for the possibility that Mb induces vascular leakage by releasing histamine from various sources in the tissue. The experiments, which were carried out on the cremaster rather than the diaphragm, as described under Methods, showed that locally injected Mb causes no vascular tattoo, hence no plasma leakage in the vascular bed of the cremaster in the Wistar-Furth rats used in our experiments. The findings were

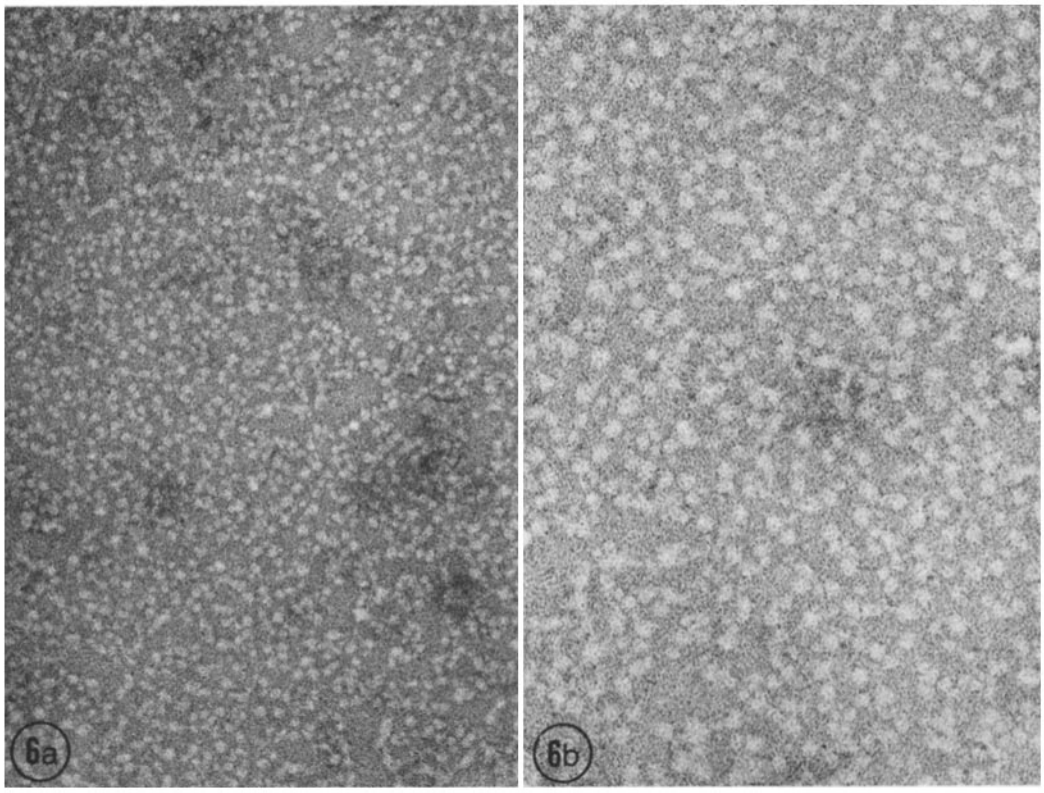

FIGURES 6 *a*, *b* Mb molecules negatively stained with 0.5% uranyl acetate oxalate at pH 7.0 in samples of the Mb peak (Fig. 5) obtained by gel chromatography of serum 10 min after the intravenous injection of the tracer solution. The large majority of the Mb molecules appears in monomeric dispersion; the few particle rows may represent aggregates formed during negative staining in the presence of small amounts of plasma proteins. (*a*) × 305,000; (*b*) × 660,000.

confirmed by light and electron microscopy which detected no intramural deposits in the small vessels of the cremaster after local Mb injections. Moreover, no intramural deposits were observed in the vasculature of the diaphragm after intravenous Mb injection.

Diffusion of Mb and Its Reaction Product into the Tissue

We also checked for Mb diffusion in the tissue by either fixing diaphragm specimens in aldehydes (see Methods) containing 0.2% Mb, or carrying out the cytochemical reaction with 0.2% Mb in the incubation medium (the latter is also a control for the diffusion of the reaction product into the tissue). In both cases, the specimens were processed through a peroxidase reaction. No reaction product was detected in either cells or interstitia along the interface of the tissue with the Mb solution. On the strength of these findings we concluded that under our experimental conditions Mb can be used as an adequate probe of the normal pathways of the capillary wall.

Pathways of Mb across the Capillary Wall

GENERAL: The basic information for this part of the work was collected from observations made on a large number of specimens (see Materials) and from counts and measurements done on 12–14 sections of capillaries from 8 different animals for each time interval given in Table I. An aggregate endothelial volume of 10.8 μm^3 comprising a total population of ~6,660 vesicles was used for the data presented in Figs. 16, 17, and 18.

Observations made in vivo on the exposed cremaster show that there is a lag of 25–30 s be-

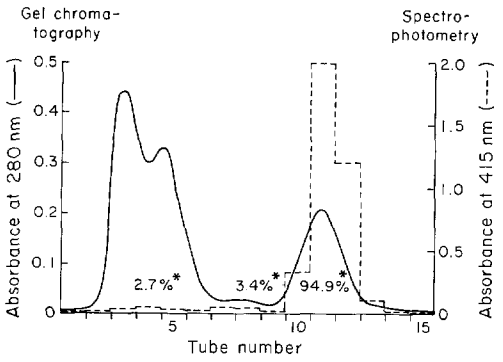

FIGURE 7 Gel chromatography (Sephadex G-75) and spectrophotometry (at 415 nm) of a rat serum sample (0.2 ml) to which was added, in vitro, 2.5 mg Mb in 0.05 ml isotonic saline at pH 7.0. * The figures are percentages of absorbance at 415 nm.

tween the beginning of fixation and the arrest of circulation in the vascular bed of the muscle. We have assumed that a similar lag applies for the diaphragm[5] and accordingly the time points given in the text and Table I have been corrected as follows: the earliest time point obtained by injecting simultaneously the tracer in the blood stream and the fixative in the pleural and peritoneal cavities is taken as 30 s past 0 time, and the time point made by injecting the fixative 45 s after the tracer is equated with 75 s past 0 time. Most observations were made during this period (30–75 s) which was covered systematically with numerous time points at intervals of 5 s or less.

Within each time interval, there is variation from one capillary to the next, but there is less variation from one interval to another so that the emerging picture applies to the large majority of the vessels observed.

Mb Behavior in Capillaries

LUMEN: From the earliest time points, the cytochemical reaction gave a product of high density and even distribution throughout the plasma, probably reflecting an even Mb distribution. The intensity of the reaction began to decrease by 10 min.

[5] Its muscle layer is slightly thicker than that of the cremaster, but the fixative diffuses into it from both sides. Hence, the time needed for the arrest of the blood flow may be the same or shorter.

Capillary Wall

ENDOTHELIUM: For the convenience of the description, we have divided the interaction of our probe with the endothelium in four phases of unequal duration, which appear to represent resolvable steps in Mb transport. In addition, we have adopted from (1) the division of the total vesicle population of the endothelium into three groups: the first associated with the blood front, the second located in the interior of the cytoplasm, and the third found along the tissue front of the cells. In part, the division is admittedly arbitrary: it relies primarily on location within or beyond ~80 nm from each front; it becomes difficult and often breaks down when the endothelium thins out to less than ~250 nm; and it is not directly related to the condition (open or closed) of individual vesicles in each group. It implies, however, a high probability of interaction with the respective aspect of the plasmalemma for each front group, and of transit through the cytoplasm for the inner group.

Finally the description of changes occurring during the four phases mentioned will be limited to two regions of the endothelial cells which appear to be particularly active, i.e., the peripheral zone and the perinuclear cytoplasm. The remaining regions will be covered later in a separate section.

PHASE I (0–35 s): In the peripheral zone of the cells, phase I is characterized by extensive vesicle labeling on the blood front, incipient marking on the inner group, and absence of reaction product in the vesicles associated with the tissue front, the percentage of labeling within the first two groups being 73% and 16%, respectively (Fig. 8). The dominant event of this phase seems to be Mb diffusion from the plasma into the vesicles of the blood front, since ~90% of those labeled within this group are open to the lumen. In some of the latter the reaction product is less dense than in the plasma, which suggests that equilibrium in Mb concentration between the plasma and these vesicles has not yet been reached.

The situation is similar for the perinuclear cytoplasm except that the percentage of labeling in the inner group is slightly lower (~10%) (Figs. 17 and 18). By the end of this phase, approximately one-third of the total vesicle population is labeled in each of the two regions (Fig. 16). Reaction product fills the shallow infundibula leading to the intercellular junctions of the endo-

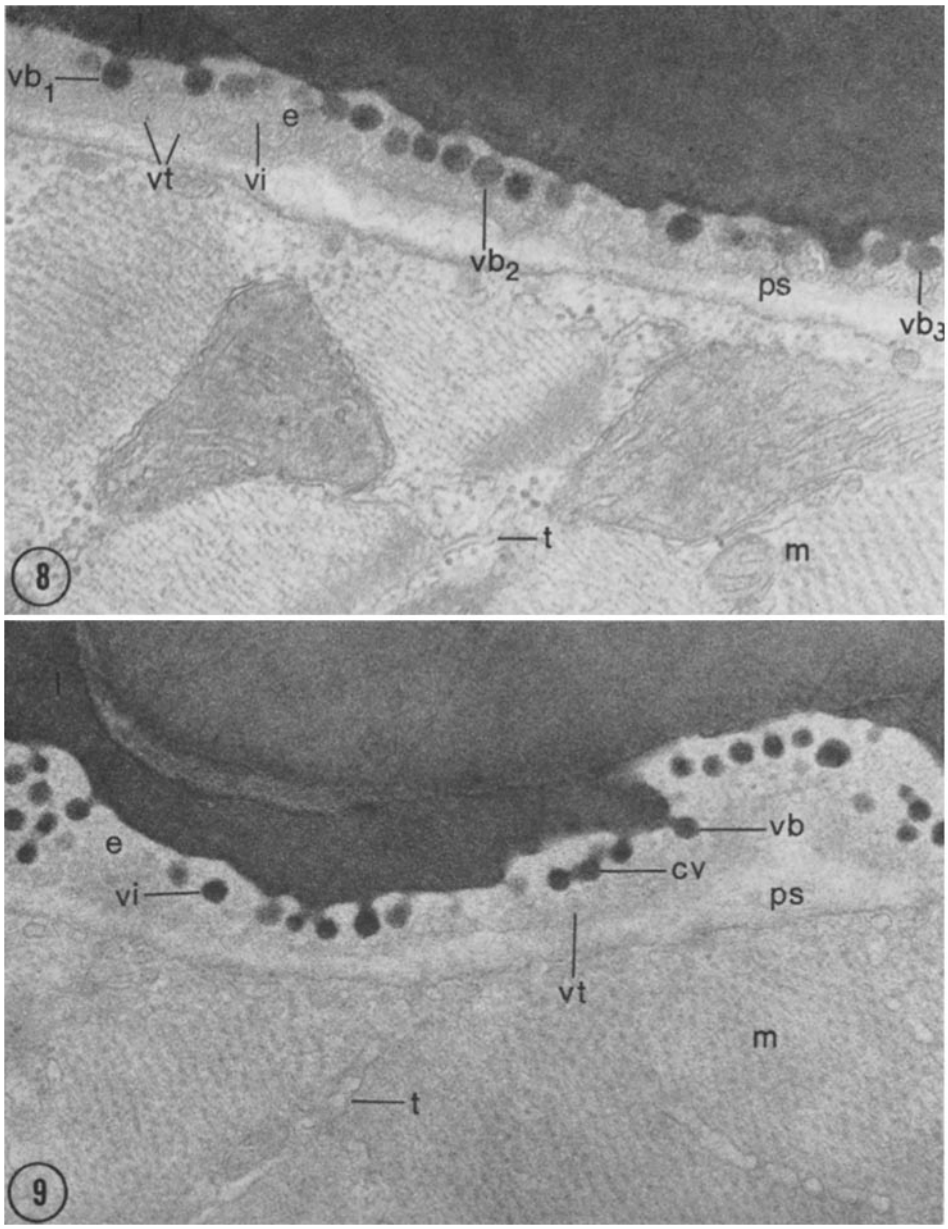

FIGURE 8 Rat diaphragm. Blood capillary 35 s after an i.v. Mb injection (phase I). The product of the Mb peroxidase reaction is present in the capillary lumen (*l*) and within most of the plasmalemmal vesicles associated with the blood front (vb_1) of the endothelium (*e*). The majority of the labeled vesicles are open to the lumen. Note that some of these vesicles (vb_2 and vb_3) contain reaction product in a concentration lower than in the adjacent blood plasma. The vesicles located inside the cytoplasm (*vi*) or on the tissue front (*vt*) are still unmarked. The pericapillary space (*ps*) is free of detectable tracer. × 40,000.

FIGURE 9 Rat diaphragm. Blood capillary 45 s after an i.v. Mb injection (phase II). Concomitantly with the labeling of many plasmalemmal vesicles on the blood front (*vb*) of the endothelium (*e*), there is appreciable marking of the vesicles of the inner group (*vi*). At this time point the vesicles on the tissue front (*vt*) are still unmarked. A chain of four vesicles is indicated by *cv*. The pericapillary space (*ps*) is free of reaction product. × 40,000.

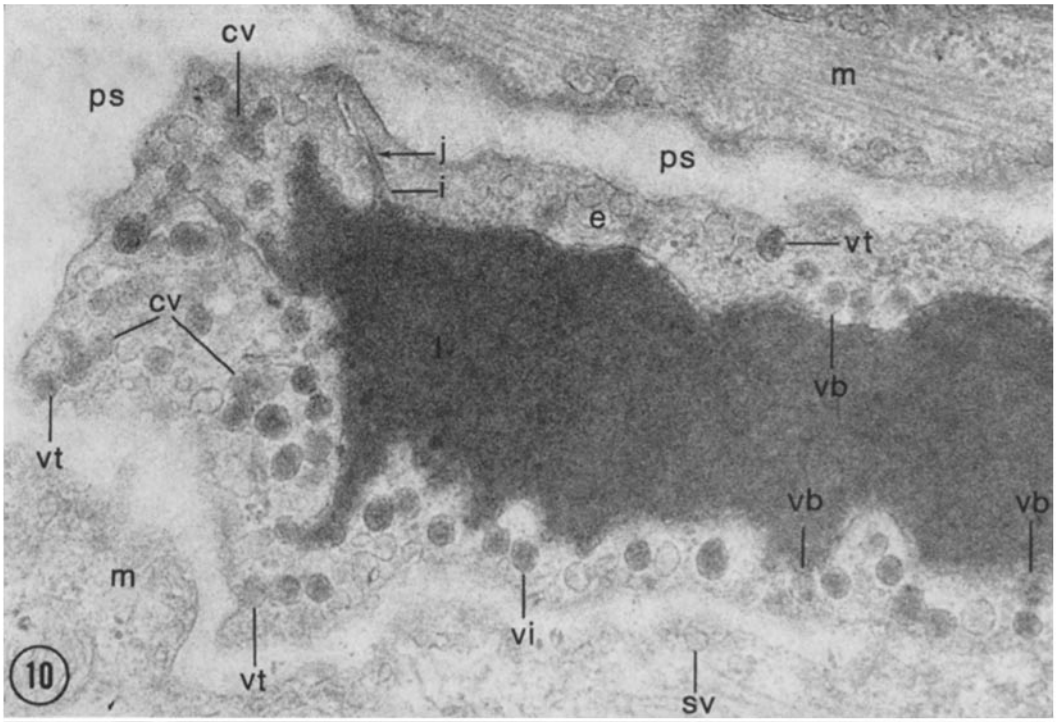

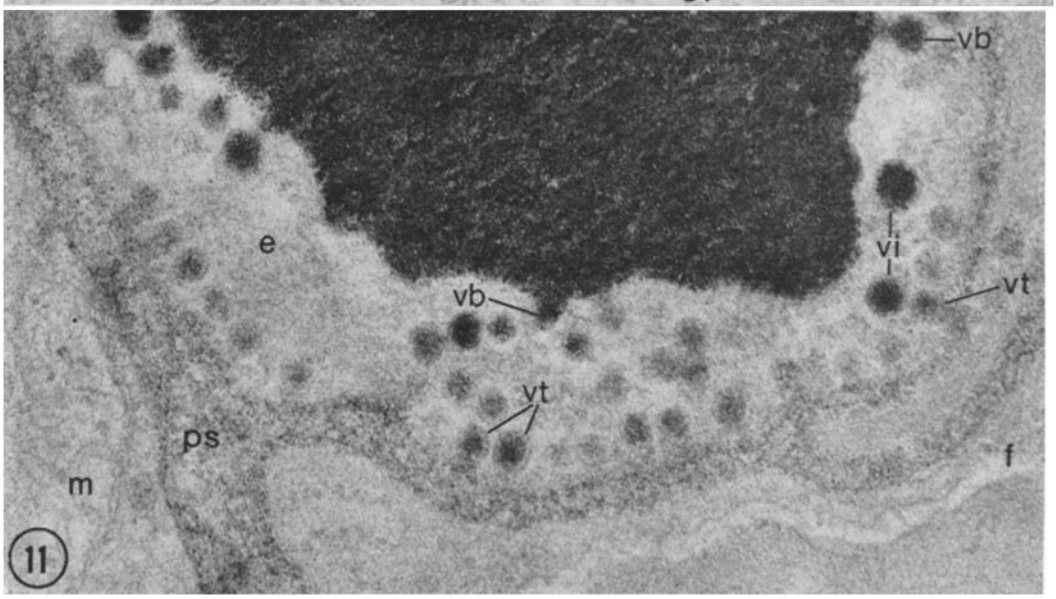

FIGURE 10 Rat diaphragm. Blood capillary 55 s after an i.v. Mb injection (phase III). Most of the plasmalemmal vesicles on the blood front (*vb*) and inside the cytoplasm (*vi*) are labeled by reaction product, while those on the tissue front (*vt*) are only partly marked. Some of the latter appear in contact with the plasmalemma but not yet open to the extracellular space. The pericapillary space (*ps*) is free of reaction product. Note the frequency of the chains of vesicles (*cv*). The infundibulum (*i*), leading to the intercellular junction (*j*) contains reaction product but the intercellular space beyond the junction is not labeled. × 50,000.

FIGURE 11 Rat diaphragm. Blood capillary 75 s after an i.v. Mb injection (phase IV). Note the extensive labeling of the plasmalemmal vesicles belonging to the three groups: on the blood front (*vb*), inside (*vi*), and on the tissue front (*vt*) of the endothelium (*e*). Many of the latter appear to be discharging. Note that their content is more heavily marked than the pericapillary spaces (*ps*) which are filled with randomly distributed reaction product. × 40,000.

thelium, but does not penetrate beyond them (Figs. 21 *a*, 22 *a*, 23 *a* and *b*).

PHASE II (35–45 s): In the peripheral zone, labeling within the first group increases slightly (up to ~75%) while that of the inner vesicles reaches ~56%; the vesicles on the tissue front are still free of reaction product (Fig. 9). The same applies for the perinuclear cytoplasm except that vesicle labeling in the inner group rises sharply to ~70% (Figs. 17 and 18).

About half of the total vesicle population is now marked by reaction product in both regions (Fig. 16). The situation of the junctions is unchanged (Figs. 23 *c* and *d*).

PHASE III (45–60 s): At the periphery of the cell, labeling percentage increases slightly for the first two groups (to 80% and 65%, respectively) and strikingly (to 30%) for the group on the tissue front. Half of the marked vesicles of this group are opened and apparently already discharging in the subendothelial and pericapillary spaces (Figs. 10, 21 *b*), as indicated by the fact that the density of the reaction product within open vesicles is often higher than in the immediately adjacent extracellular space. In the perinuclear cytoplasm the labeling follows the same course with even higher percentages within each group (Figs. 17 and 18). Two-thirds of the total vesicle population are now labeled in each of the two regions (Fig. 16).

PHASE IV (60–75 s): In both regions, each vesicle group and hence the total vesicle population is found labeled to nearly the same high extent (~80%) (Figs. 16, 17, 18). A large percentage of the marked vesicles of the third group are open and apparently discharging on the tissue front (Figs. 11, 12) and reaction product is now present in varied concentration throughout the pericapillary spaces (Figs. 13, 14, and 24).

The infundibula leading to the junctions are marked heavily and to the same extent as the plasma. The junctions proper are not labeled, but the intercellular spaces past the junctions are generally marked (Figs. 14, 22 *b*, and 23 *e*), the concentration of reaction product within these spaces being equal to, or lower than, that seen in the adjacent pericapillary spaces (Figs. 14, 22 *b*). Labeled vesicles are occasionally found open to the cell surface in the abluminal part of the intercellular spaces (Figs. 21 *b*, 22 *b*, and 23 *e*). During phase III the situation of the junctions varies from capillary to capillary between appearances described above for phase II and phase IV.

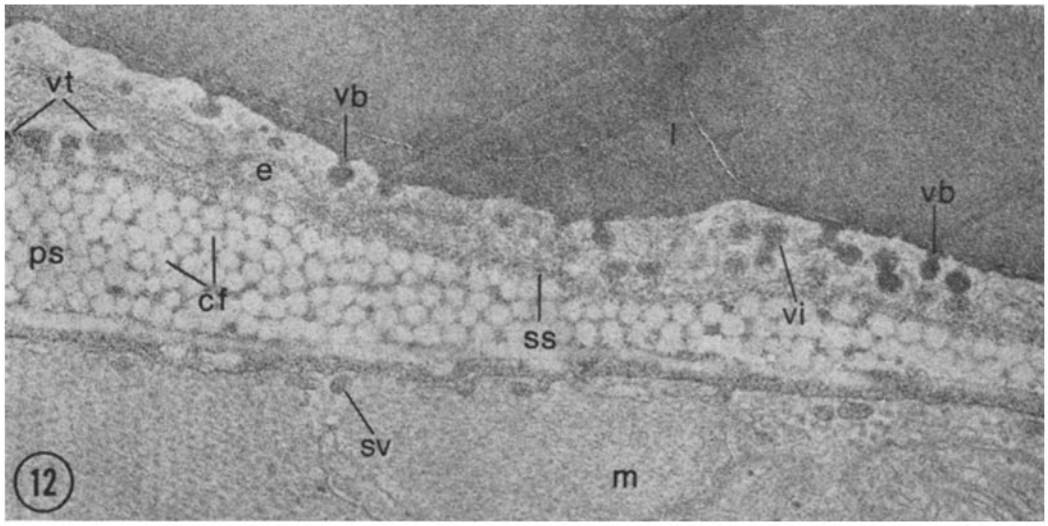

FIGURE 12 Rat diaphragm. Blood capillary 75 s after an i.v. Mb injection (phase IV). Reaction product is present in the plasmalemmal vesicles belonging to the three groups: on the blood front (*vb*), inside (*vi*) and on the tissue front (*vt*) of the endothelium (*e*). Most of the vesicles in the last group are open to the subendothelial space (*ss*). Reaction product marks the basement membrane of the capillary, the interfibrillar matrix around collagen fibers (*cf*) in the pericapillary spaces (*ps*), and the basement membrane of the muscle fiber (*m*); it also labels the sarcolemmal vesicles (*sv*) of the latter. × 40,000.

In all four phases, a small fraction of the total vesicle population is organized in short chains of 2–4 vesicles (Fig. 15) which often extend from one vesicular group to its neighbor, but apparently do not form connecting channels between the two fronts of the endothelium.

LATER TIME POINTS: Past phase IV we have examined a series of specimens fixed at time

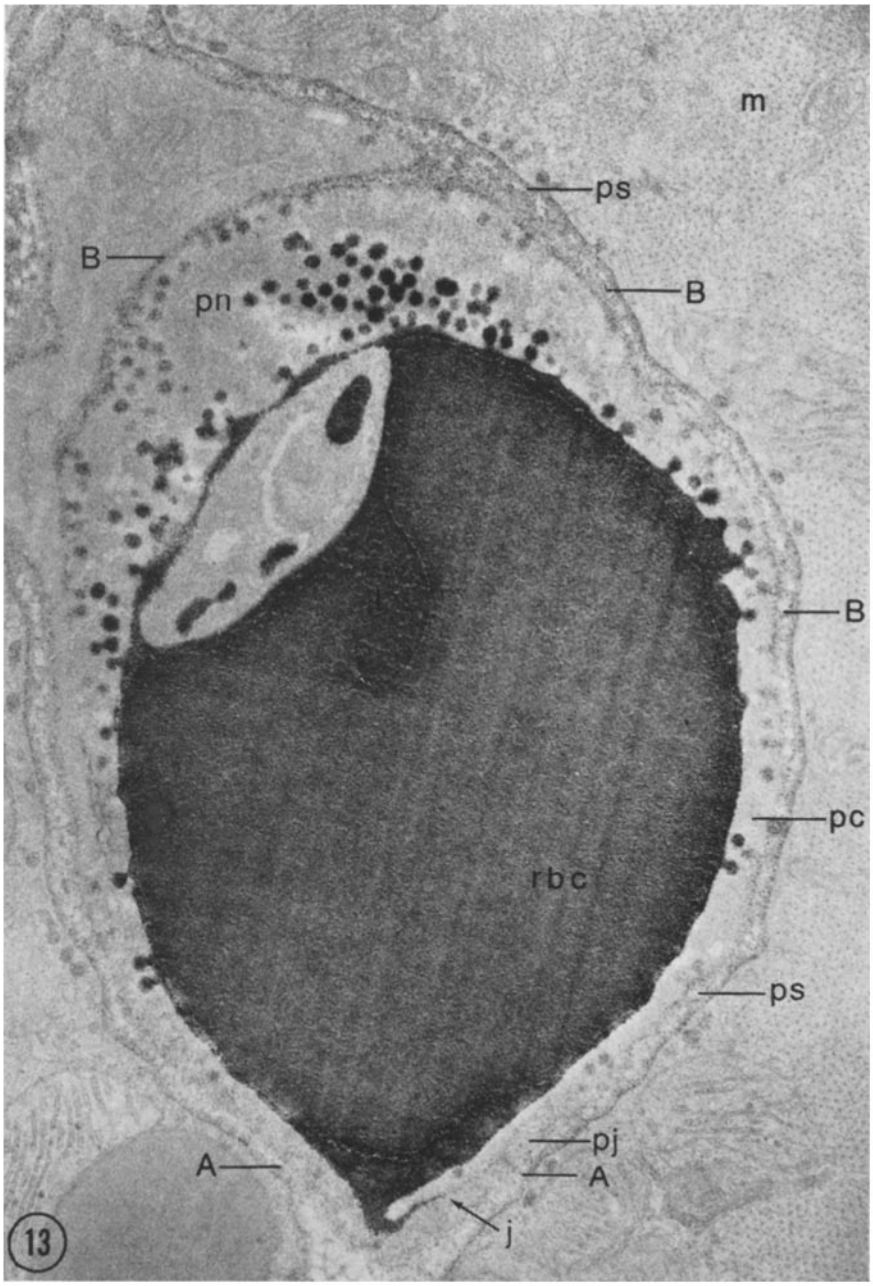

FIGURE 13 Rat diaphragm. Blood capillary 90 s after an i.v. Mb injection. Except for the parajunctional zone, the other zones of the endothelium contain marked vesicles in all three positions. In the pericapillary spaces (*ps*), the density of the reaction product is lower within the sector *A* facing the parajunctional zone than within the sector *B* corresponding to other endothelial regions. × 30,000.

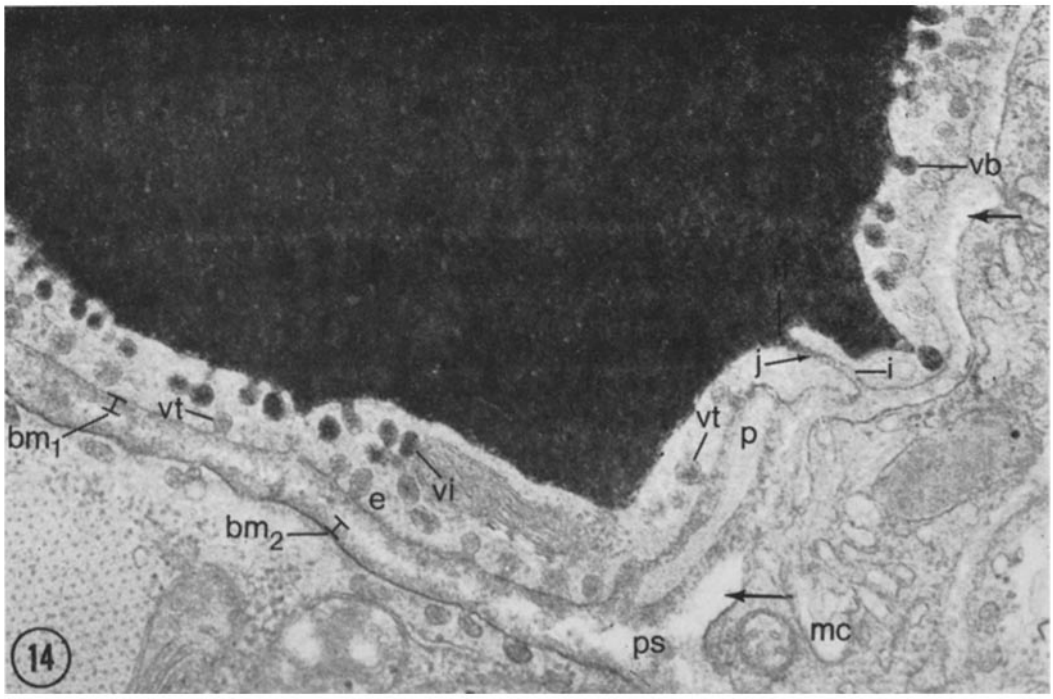

FIGURE 14 Rat diaphragm. Blood capillary 75 s after an i.v. Mb injection. The percentage of labeling is high for vesicles in all three positions, on the blood front (*vb*), inside (*vi*), and the tissue front (*vt*) of the endothelium (*e*). Reaction product appears preferentially concentrated within the basement membranes of the capillary (bm_1) and muscle cell (bm_2), while the capillary space around the macrophage at (*mc*) is practically unlabeled (arrows). Reaction product fills the infundibulum (*if*) leading to the intercellular junction (*j*) at a concentration comparable with that in the lumen, but in the intercellular space (*i*) beyond the junction it occurs in a concentration equal to that in the adjacent pericapillary spaces (*ps*). × 50,000.

points extending up to 4 h. The percentage of labeling in the different groups and in the total vesicle population remains stable at $\lesssim 90\%$. Past 10 min the reaction product appears to reach the same density in the lumen, the plasmalemmal vesicles, the intercellular spaces of the endothelium, and the interstitia of the tissue.

OTHER ENDOTHELIAL REGIONS: The pattern of vesicle labeling showed significant regional heterogeneity among the four parts we have distinguished within endothelial cells. In contradistinction to the two active regions we have already described (i.e., the peripheral zone and the perinuclear cytoplasm), the narrow parajunctional zone characterized by a generally low vesicle frequency appears relatively inactive. Vesicles of this zone are involved in the marking of the abluminal parts of the intercellular spaces of the endothelium (Figs. 21 *b*, 22 *b*, and 23 *e*).

The organelle region, which has only one-third the frequency of vesicles of the peripheral zone, lags behind in Mb uptake; only 20% of the vesicles on its blood front are labeled at the end of phase I as compared with >70% for the peripheral zone and the perinuclear cytoplasm (Figs. 19 and 25 *a*, *b*). The overall involvement of the region's total vesicle population is also more limited: at the end of phase IV its labeling percentage is 56% as opposed to ~80% for the two active regions.

ASYMMETRIES: In a small number of capillaries (~5% of the profiles examined) we have encountered a striking asymmetry in the pattern of vesicle labeling. Through phase I and II, and only occasionally through phase III, endothelial sectors with labeled and unlabeled vesicles are found on the same capillary profile (Fig. 20). These sectors are generally large (~3–4 μm, 2–3 per profile) and appear randomly distributed in relation to the cell's regions, although unlabeled

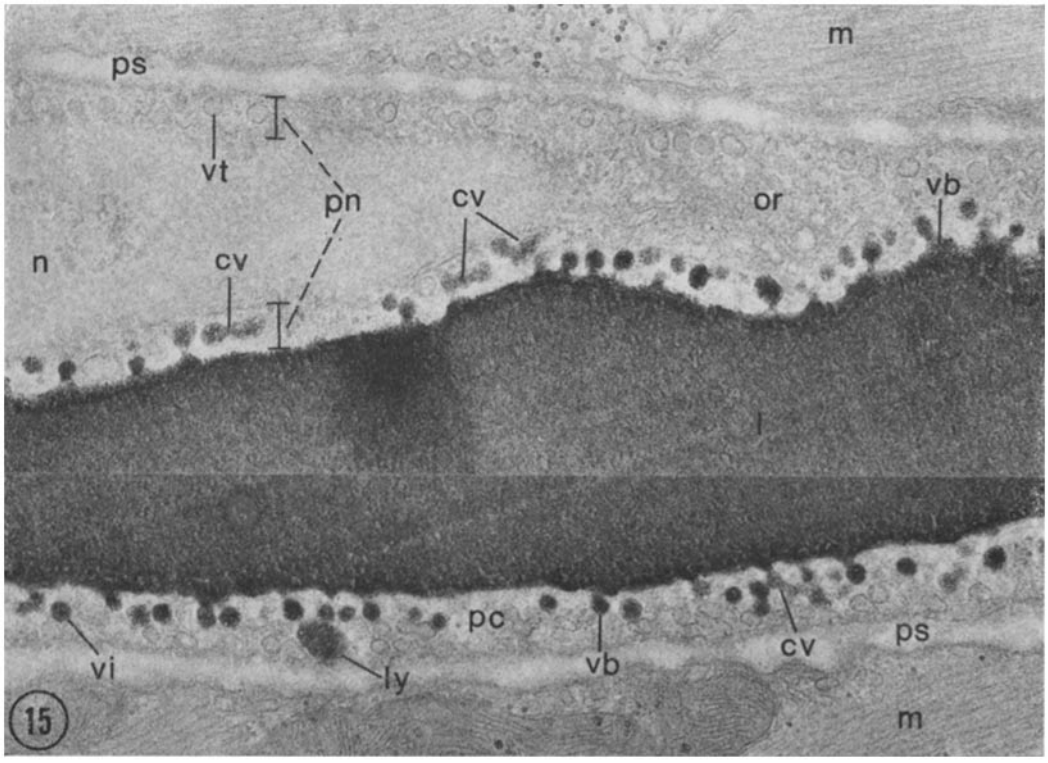

FIGURE 15 Rat diaphragm. Blood capillary 45 s after an i.v. Mb injection. Vesicle labeling has reached a similar level in the three endothelial regions shown here: the cell periphery (*pc*), the organelle region (*or*), and the perinuclear cytoplasm (*pn*). At this time point (Phase III) no labeling of tissue front vesicles (*vt*) or pericapillary space (*ps*) occurs. Note the high incidence of chains of vesicles (*cv*). The marked structure at *ly* is probably a lysosome. × 28,000.

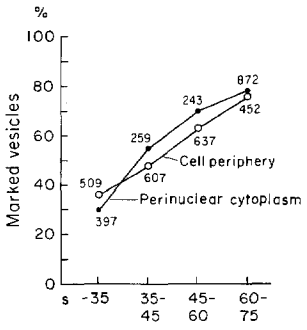

FIGURE 16 Labeling percentage in the total population of plasmalemmal vesicles at different time intervals. The figures give the number of vesicles counted.

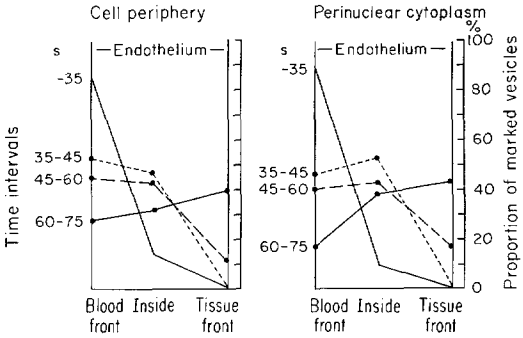

FIGURE 17 Total population of marked vesicles: its distribution among the three groups of plasmalemmal vesicles in the cell periphery and in the perinuclear cytoplasm, as a function of time.

sectors seem to coincide more frequently with parajunctional zones. The organization of the endothelium in such capillaries appears to be normal. The phenomenon may be caused by incomplete mixing of Mb in the plasma, which in turn may reflect irregular flow in individual capillaries (59).

Mb ACCESS TO OTHER CELL COMPARTMENTS: Throughout the period within which

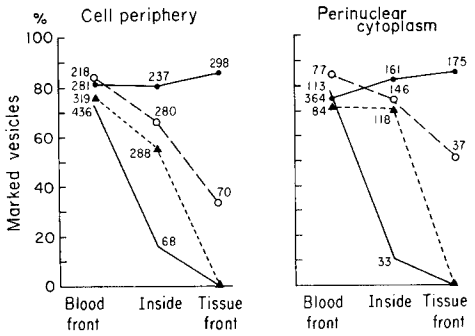

FIGURE 18 Labeling percentage in the three groups of plasmalemmal vesicles in the cell periphery and in the perinuclear cytoplasm at different time intervals: —— up to 35 s; ▲---▲ at 35–45 s: O---O at 45–60 s; ●——● at 60–75 s. The figures give the numbers of vesicles counted.

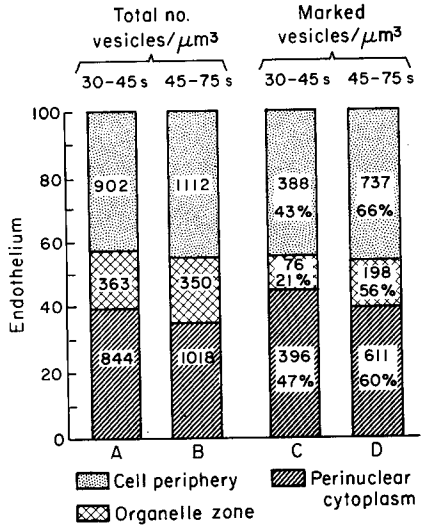

FIGURE 19 Average frequency of vesicles and marked vesicles per cubic micron in three of the four endothelial zones. Percentage distribution of endothelial volume is given by the ordinate (absolute figures available in Simionescu, Simionescu, and Palade, manuscript in preparation). The columns in this graph represent (*a*) the average volume occupied by the first three zones; (*b*) their respective content in total number of vesicles (*A* and *B*); (*c*) their content of marked vesicles (*C* and *D*) as a function of time. Columns *A* and *B* show that during Mb transport the vesicle distribution between the three zones remains the same but their frequency increases by 17% from the first (phases I and II) to the second interval (phases III and IV). Columns *C* and *D* show that during the second interval the absolute number of marked vesicles increases in the three regions and especially in the organelle region, in which the highest relative increase is also recorded. The figures on bars *A* and *B* give the frequency of plasmalemmal vesicles (total number of vesicles/cubic micron) in each region at two intervals during Mb transport. The figures on bars *C* and *D* give the frequency of labeled vesicles (number of labeled vesicles/cubic micron) for the same regions and intervals. For each region and each interval the percentage of vesicle labeling (e.g., $C/A \times 100$) is also given. The endothelial volumes surveyed for the data in the graph were: cell periphery and organelle region, 3.03 μm^3 for the interval 30–45 s and 3.32 μm^3 for the interval 45–75 s; perinuclear cytoplasm, 2.21 μm^3 for the first interval and 2.19 μm^3 for the second.

the tracer can be detected in the plasma (i.e., up to 4 h) reaction product was found restricted to plasmalemmal vesicles. There was no labeling of any other membrane-bounded cytoplasmic compartment, e.g. the endoplasmic reticulum, the nuclear envelope, or the Golgi complex (Figs. 25 *a*, *b*), and no labeling of the cytoplasmic matrix; the only exception was a few lysosomes and even in this case the amount and concentration of reaction product they contained were negligible by comparison with those found in plasma, vesicles, and pericapillary spaces.

BASEMENT MEMBRANE: During and past phase III, we did not detect any accumulation of reaction product against the basement membrane in the subendothelial space; we found instead that the reaction spreads very rapidly past the basement membrane into the pericapillary spaces. At the beginning of phase III, and occasionally through phase IV and later, the basement membrane of the capillary wall seems to be more heavily stained by the reaction product than the adjacent spaces, suggesting that Mb is partially retained within this membrane. The basement membrane of muscle fibers behaved in the same way (Figs. 13 and 14).

The plasmalemmal vesicles of the pericytes were labeled but there was little or negligible staining of phagosomes or lysosomes in these cells.

ADVENTITIA AND PERICAPILLARY SPACES: From the beginning (phase III), the distribution of reaction product in the adventitia of the vessels and in the pericapillary spaces was uneven. The collagen fibrils appeared in negative contrast, due to an apparent concentration of reaction product in the interfibrillar matrix, and other local variations were encountered without evident connection with the cellular or fibrillar elements of these regions.

There was negligible staining of the phagosomes and lysosomes of macrophages and fibroblasts, but

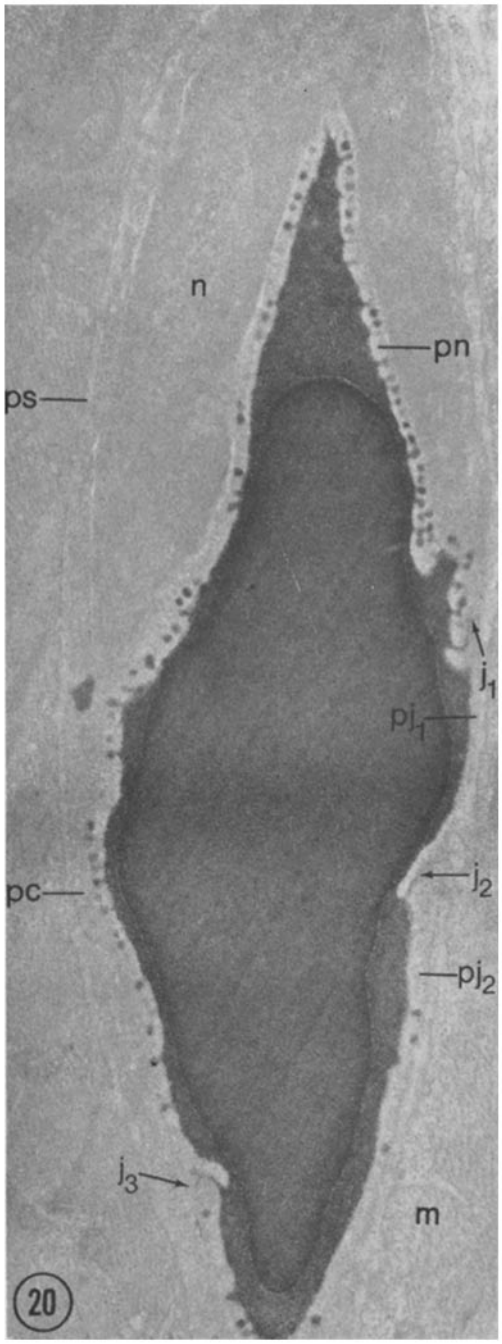

FIGURE 20 Rat diaphragm. Blood capillary 35 s after an i.v. Mb injection (phase I). Asymmetric labeling involving only the vesicles of the perinuclear cytoplasm (*pn*) and part of the cell periphery (*pc*). The unlabeled sectors are centered on two parajunctional zones (pj_1 and pj_2). × 18,000.

there was detectable staining of the T system and plasmalemmal vesicles of adjacent muscle fibers. There was even a suggestion of concentration in these vesicles, as well as in those of the pericytes (Fig. 26), and some indication that the density of the plasmalemma of muscle fibers is increased by the staining. No comparable increase in density was noted for the plasmalemma of the pericytes and endothelial cells.

During phase III (Fig. 24) and phase IV (Fig. 13) we occasionally encountered concentration gradients of reaction product around the endothelium in the basement membrane and the adjoining pericapillary spaces. Their maxima were centered on vesiculated regions of the endothelium, rather than on exits from intercellular spaces, and their presence was more easily detected in narrow interstitia; such gradients appeared to be transient in nature: they were no longer seen past phase IV.

DISCUSSION

Mb as Probe Molecule

The proteins with peroxidatic activity currently used as "probe" molecules in investigating capillary permeability are detected indirectly via the products of their cytochemical reactions. This approach takes advantage of the large amplification step from enzyme to reaction product, but cannot by itself ascertain the nature or size of the molecule(s) actually involved in the reactions. Hence, a reliable interpretation of the results obtained requires the demonstration that: (*a*) the probe retains its dimensions throughout the experiment, and (*b*) no other significant peroxidatic activity exists in the experimental tissue.

In our work, we have demonstrated by gel filtration on Sephadex G-75, spectrophotometry, and electron microscopy of negatively stained specimens that the probe we have used, e.g., Mb exists in uniform monomeric dispersion in the solutions to be injected. The same applies for the Mb injected into the blood stream and examined in the plasma at intervals longer than required (10 min) for the significant part of our observations. There is no, or negligible, binding to plasma proteins,[6] no significant aggregation or polymeri-

[6] In the case of HRP, the evidence bearing on this point is limited and contradictory. Some reports indicate that the enzyme does not bind to plasma proteins, but changes in molecular weight cannot be excluded (60); others, that it appears in the β-globulin and

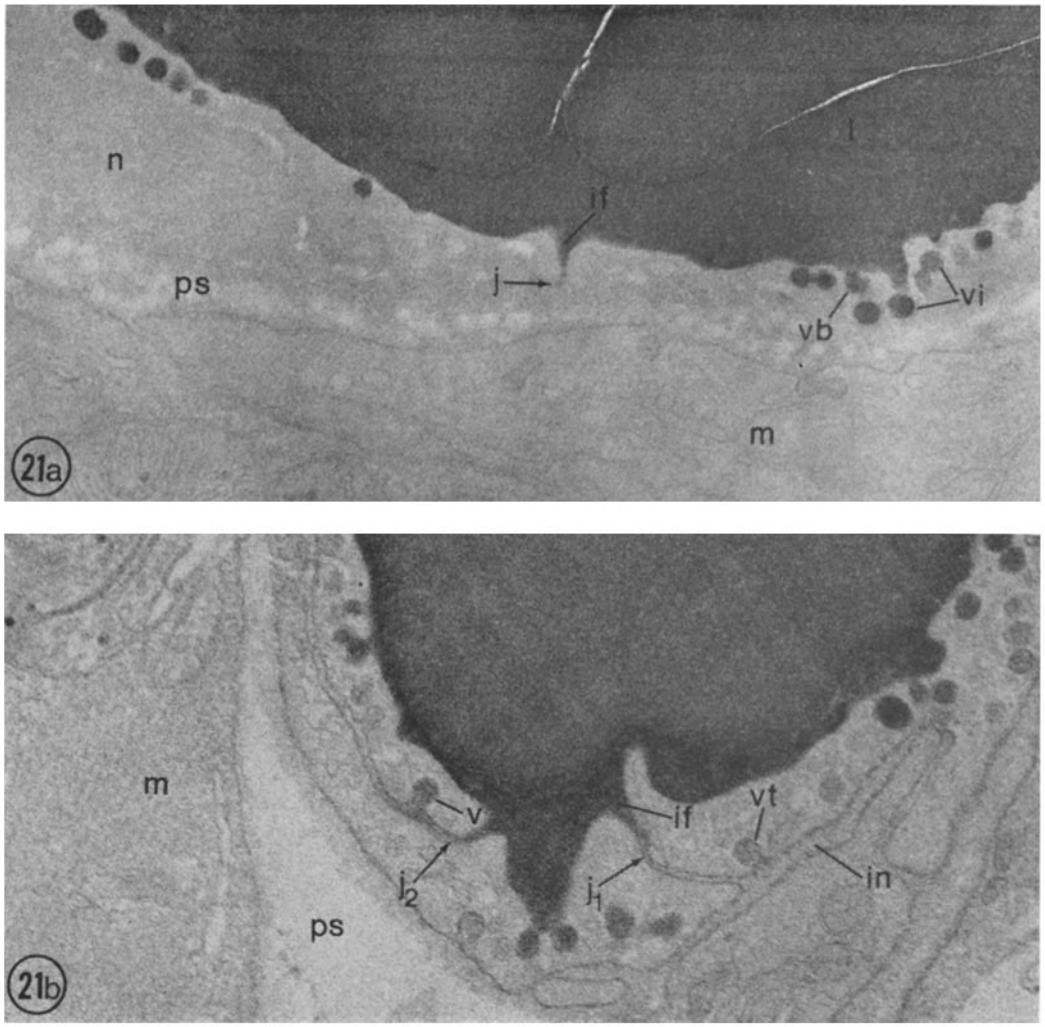

FIGURES 21 *a*, *b* Intercellular junctions of the endothelium at different intervals after an i.v. Mb injection. (*a*) at 35 s (phase I). Reaction product is present only within the infundibulum (*if*) leading to the intercellular junction (*j*). (*b*) At 50 s (phase III). The intercellular space past junction j_1 appears free of reaction product, while discharge of labeled vesicles (*vt*) on the tissue front is in progress. A vesicle (*v*) unloads its content in the intercellular space behind a second junction marked j_2. × 40,000.

zation, and no detectable degradation of the tracer. In this respect, our results are in general agreement with data in the literature which report that Mb is stable in solution over a wide range of concentration (13–16), pH (17–22), and temperature (18, 20, 23–25, 27, 28); they are also in agreement with specific observations which show that Mb does not bind to plasma proteins (62–64).

In addition, we have demonstrated that there is no other source of peroxidatic activity in the plasma, except for a negligible amount of hemoglobin which leaks from erythrocytes, as a result of a slight degree of hemolysis induced by the fixative. The finding is in agreement with observations made by using ^{59}Fe-labeled hemoglobin (65). Finally, we have shown that Mb does not induce

IgG fractions (61); finally, others mention that the sera of both HRP injected and noninjected mice have a faint peroxidase positive band migrating with the albumin band (4).

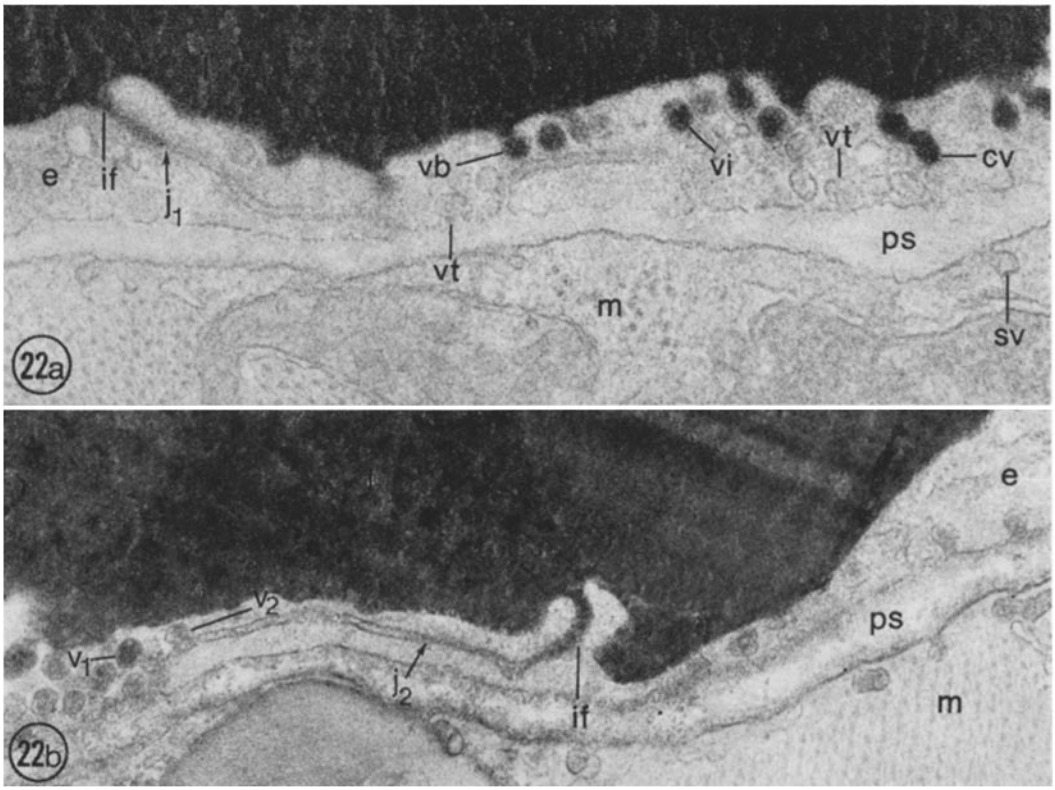

FIGURES 22 *a, b* Intercellular junctions of the endothelium at different time points after an i.v. Mb injection. (*a*) at 30 s (phase I); (*b*) at 45 s (phase II). The long, tortuous intercellular spaces beyond junctions j_1, j_2 appear free of reaction product except for the end of the space in *b* in which two plasmalemmal vesicles (v_1, v_2) are discharging. (*a*) × 32,000; (*b*) × 40,000.

abnormal permeability (vascular leakage) in muscle capillaries.

On the strength of the results obtained in these prerequisite experiments, we conclude that Mb is an adequate molecular probe, and we assume that our findings reflect the interaction of individual Mb molecules with the normal passageways extant in the wall of muscle capillaries. As is well known, the current physiological literature (66–69) postulates that these passageways are pores that belong to two distinct categories: large ($d \simeq 500$ Å) and small ($d \simeq 90$ Å) and considers as an alternative for the latter, the existence of slits open to a gap of 40–50 Å and located in the intercellular junctions of the endothelium.

On account of its dimensions (25 × 34 × 42 Å, or 33 $Å_{avg}$), Mb qualifies as a probe for both pore systems: it is expected to penetrate freely the large pores and to move with some restrictions, due to molecular sieving (70, 71), through the small ones. As a small pore probe, Mb has over HRP (md = 40–50 Å) the advantages of smaller size, proved homogeneity, and well-established tridimensional structure; it is, however, less active as a peroxidase (72, 73). Cytochrome *c* is slightly smaller (30 × 34 × 34 Å including side chains [10] and 25 × 25 × 37 Å disreagrading the peripheral side chains [74]), but it is 10 times less active than Mb (72); its heme is located inside the molecule in a deep cleft which presumably makes it hardly accessible to H_2O_2. In Mb, the heme is at the surface of the molecule (72, 73, 75) supposedly within easy reach for H_2O_2.

Pathway of Mb across the Capillary Wall

GENERAL: The product of the peroxidase reaction (oxidized, and polymerized diaminobenzidine [cf. 76]) is known to be highly insoluble in water and organic solvents (see, however, [77]).

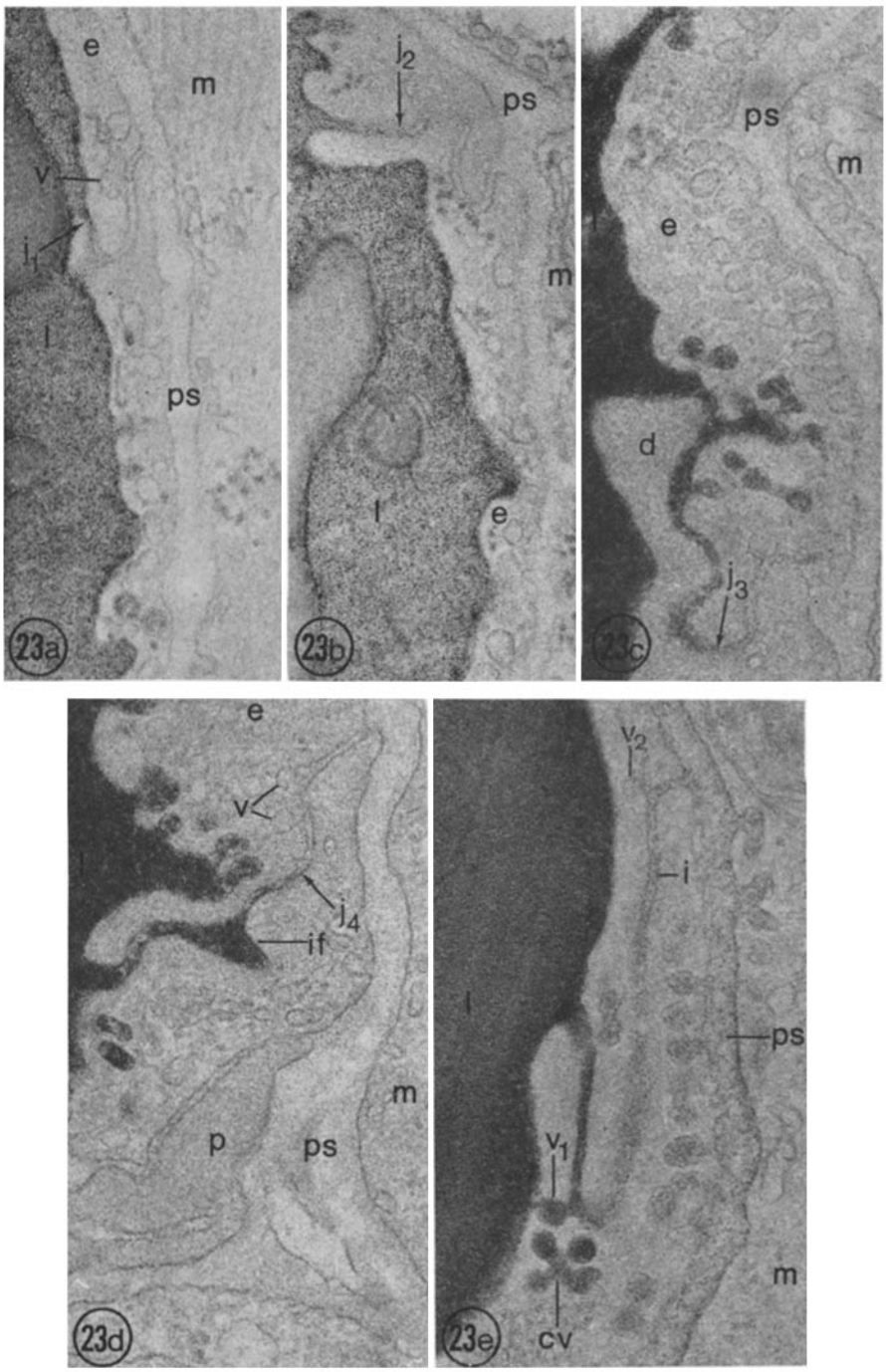

FIGURES 23 *a–e* Intercellular junctions of various geometry in blood capillaries of the rat diaphragm at different time points after an i.v. Mb injection. At 30 s (*a*) and at 35 s (*b*), at the beginning of vesicles labeling the intercellular spaces behind junctions j_1 and j_2 are free of reaction product. Behind j_1 an unmarked vesicle (*v*) opens in the intercellular space. At 40 s (*c*) the partially collapsed lumen of a capillary forms a complex diverticulum (with numerous associated labeled vesicles) which leads to junction j_3. The intercellular space beyond the latter is not labeled. At 40 s (*d*) an oblong marked infundibulum (*if*) leads to junction j_4. The space beyond it is not labeled. Note that two unmarked vesicles (*v*) open in this space. At 65 s (*e*) the position of the junction along this long intercellular space cannot be ascertained (the section is oblique). Vesicles are opening on the proximal (v_1) as well as on the distal segment (v_2) of the space. Note the different concentration of reaction product: equal to that in the lumen in the proximal segment, and to that in the pericapillary spaces (*ps*) in the distal one. × 40,000.

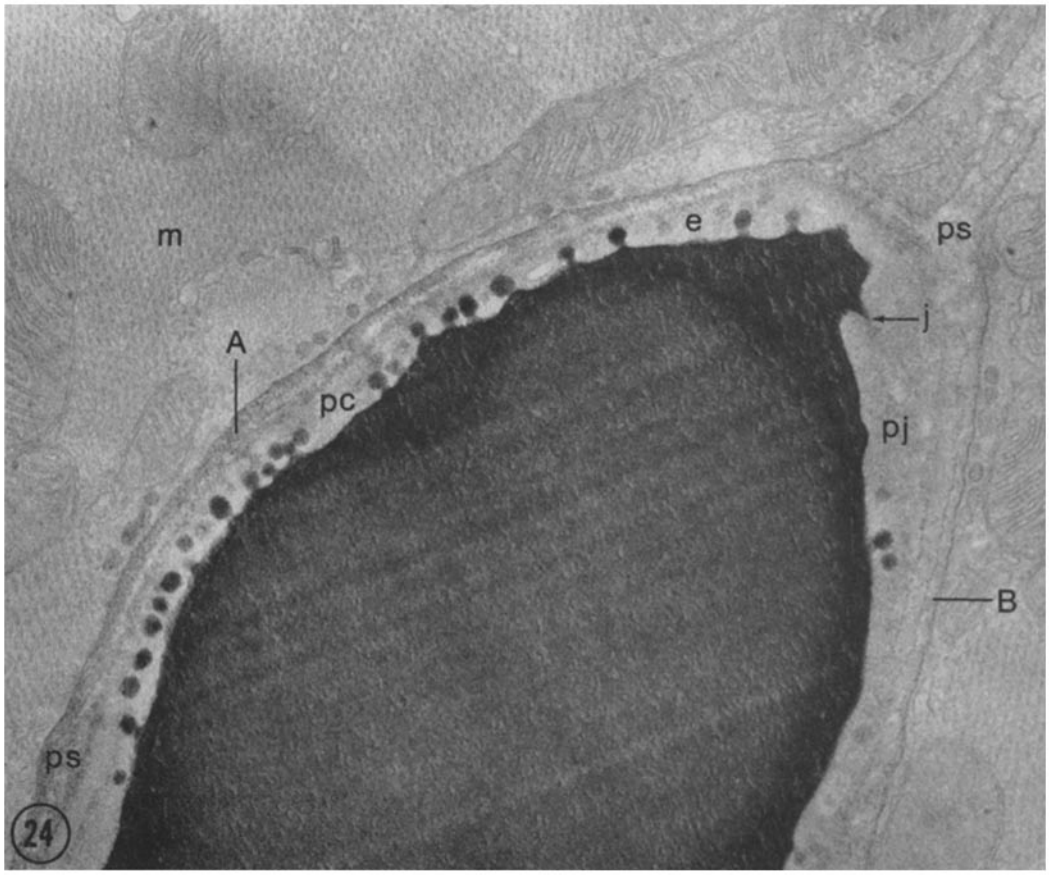

FIGURE 24 Rat diaphragm. Blood capillary 60 s after an i.v. Mb injection. Note the concentration gradient of reaction product in the pericapillary space (*ps*). The concentration is higher in the sector *A*, the part corresponding to the active cell periphery of the endothelium (*pc*) and low in the sector *B* adjacent to the less active parajunctional zone (*pj*). The position of the junction *j* is indicated by a labeled infundibulum. × 36,000.

Although we are dealing with a set of complex reactions carried out in a heterogeneous system (organized tissue), we assume at a first approximation that the location and density of the reaction product parallel the location and concentration of Mb molecules in the various compartments of the tissue. For this reason, and for the convenience of the presentation, our results will be discussed and interpreted in terms of the movement of Mb from one compartment to another, with the understanding that the actual observable is the progressive appearance of the reaction product in varied concentrations, along these compartments.

Endothelium

VESICLES: While in transit across the endothelium from the lumen to the pericapillary spaces, Mb appears definitely restricted to plasmalemmal vesicles: it cannot be detected in the cytoplasmic matrix or in any other endothelial cell compartment with the possible exception of lysosomes, to which only small amounts of the probe appear to be diverted.

From the earliest observable time point after i.v. injection, i.e. 30 s, Mb is present in a large fraction (~75%) of the vesicles associated with the blood front of the endothelial cells; 10–15 s later it is also found in a large proportion of the vesicles located in the interior of the cytoplasm; and in the subsequent 10–15 s it is detected in vesicles on the tissue front. Within this 60 s interval, the labeling of the plasmalemmal vesicles takes the appearance of a wave that moves progressively from one cell front to the other. Since we cannot detect a faster

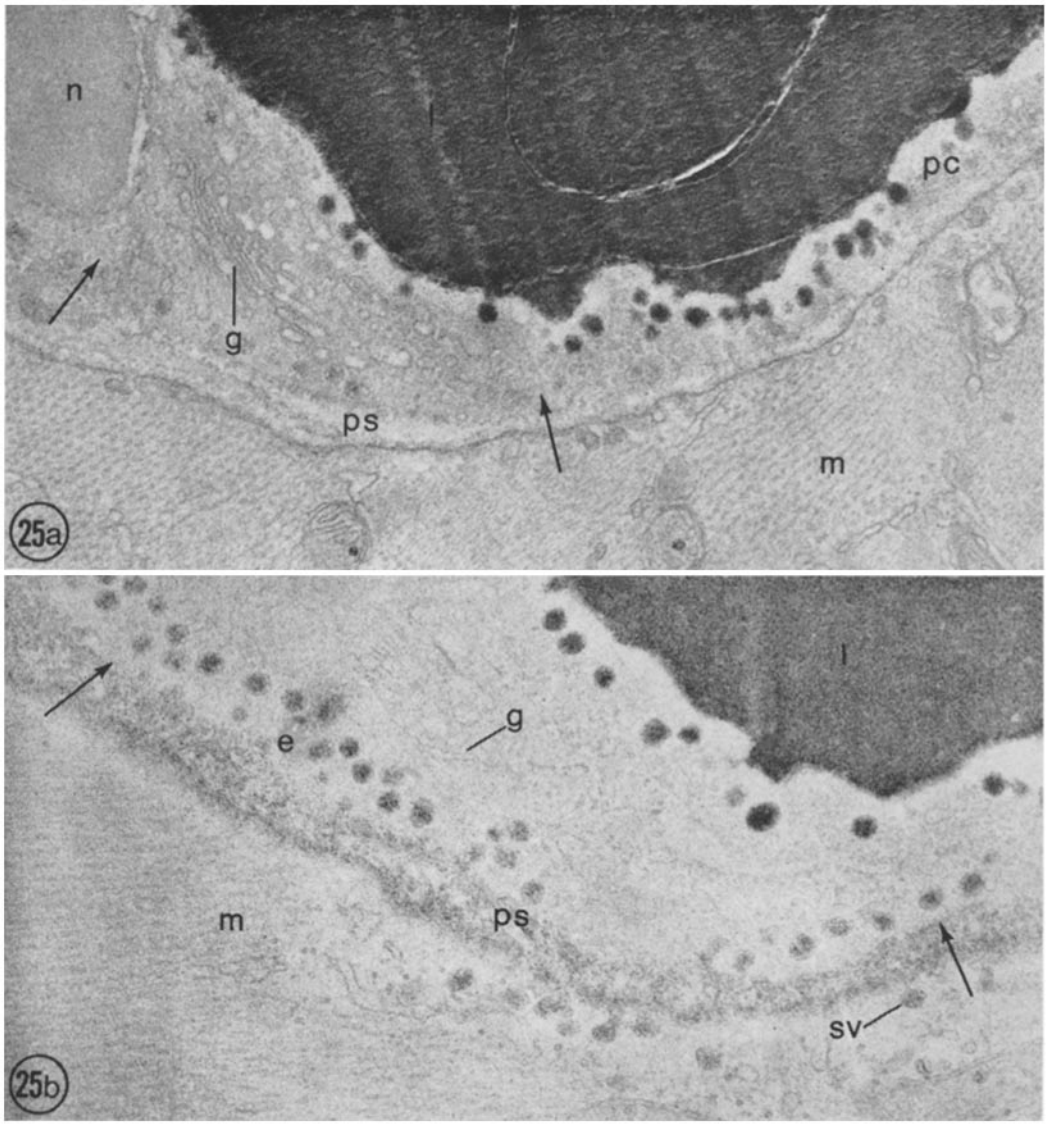

FIGURES 25 *a, b* Rat diaphragms. Blood capillaries at 45 s (*a*) and 70 s (*b*) after an i.v. Mb injection. During the earlier interval (*a*) the organelle region (between arrows) shows a limited extent of vesicle labeling restricted to the group associated with the blood front. At later time points (*b*) the percentage of vesicle labeling markedly increases, approaching that found at the cell periphery. Note the absence of labeling of the Golgi complex (*g*) of the endothelial cell and the "staining" of the sarcolemma in 25 *a*. (*a*) × 34,000; (*b*) × 42,000.

or concomitant Mb movement along the intercellular junctions, we assume that the labeling of the plasmalemmal vesicles reflects Mb transport. This assumption is supported by the presence of vesicles which are discharging on the tissue front and which are marked by reaction product in higher concentration than in the pericapillary spaces. It is also supported by the occasional detection of concentration gradients in the narrow interstitia between endothelia and pericytes or other cells; such gradients have their maxima centered on vesiculated segments of the endothelium.

Besides establishing that the plasmalemmal vesicles play a major, or possibly exclusive, role in

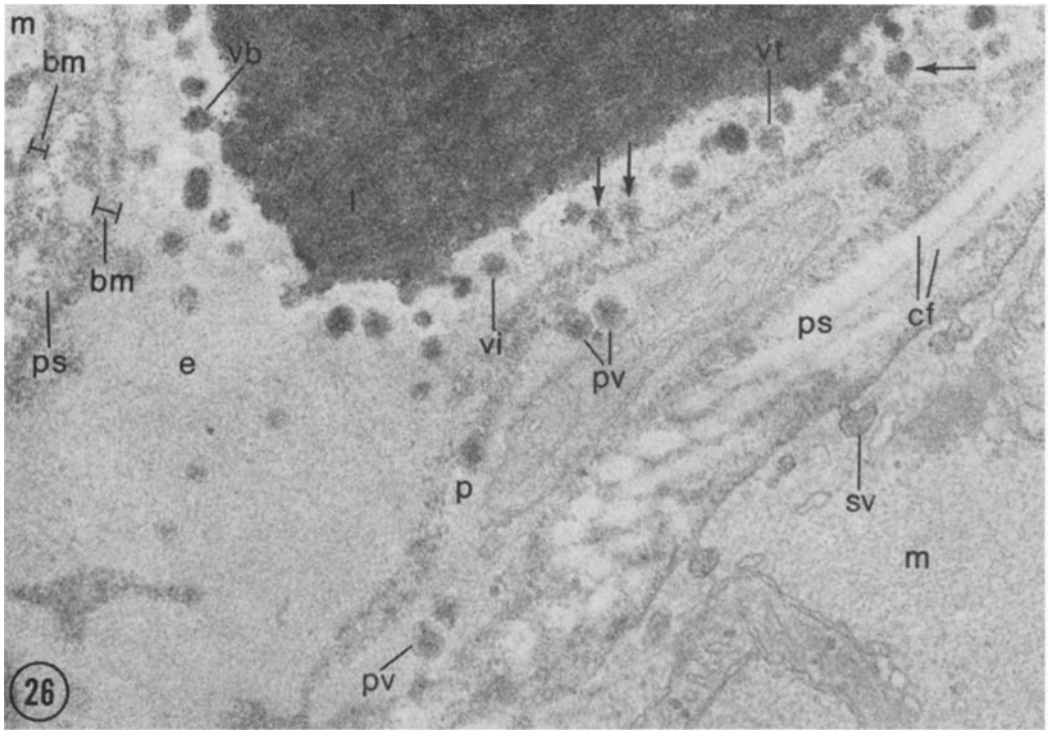

FIGURE 26 Rat diaphragm. Blood capillary 90 s after an i.v. Mb injection. Reaction product marks practically all the vesicles of the endothelium in each of the 3 groups (blood front [*vb*], inside [*vi*], and on tissue front [*vt*]). Many of the latter (arrows) are more heavily labeled than the adjacent pericapillary space (*ps*). Note the labeled plasmalemmal vesicles of a pericyte (*pv*) and the labeled sarcolemmal vesicles (*sv*) of an adjacent muscle fiber, the density of reaction product within the basement membrane (*bm*) of the capillary and of the muscle fiber, and the negative image of collagen fibers (*cf*) seen in oblique and transverse section. × 65,000.

Mb transport, our findings indicate that a large fraction of the total vesicle population partakes in this operation. Past 60 s, at a time when a steady-state condition seems to be approached, ~80% of the vesicles within each group (blood front, interior, and tissue front) are labeled.

The kinetics of labeling suggest that the different phases we have distinguished in the transport operation are of unequal duration: 30 s after the injection of Mb into the blood stream, most of the label is still restricted to vesicles associated with the blood front; this interval covers phase I. In the next 30 s, which cover phases II–IV, the probe moves across the entire endothelial layer and begins to be discharged on the tissue front. The relative slowness of phase I could be explained by a variety of factors such as: (*a*) restrictions imposed on Mb diffusion from the plasma to the vesicle content by narrow necks (1), extraneous coatings of the type stainable by ruthenium red (78, 79), or steric exclusion by other macromolecules (80); (*b*) the detachment of the vesicles from the plasmalemma may be an inherently slow operation; (*c*) this detachment, as well as the movement of detached vesicles within the cytoplasmic matrix, may be slowed down by the fixative which is expected to affect first membrane movement, then cytoplasmic viscosity and finally diffusion, simply on account of differences in concentration of cross-linkable proteins in the sites mentioned. Aldehyde penetration is fast (81, 82) and slight increases in cytoplasmic viscosity are bound to affect drastically the rate of vesicle movement within the cell (83, 84). With the information at hand, we cannot decide which of these factors accounts for the slowness of phase I.

Our recent results show that the time required for the net movement of loaded vesicles from one

cell front to the other across a 0.2–0.3 μm thick layer of cytoplasm is greater than 10 s and smaller than 25 s, and the time needed for vesicle fusion with the plasmalemma and ensuing discharge on the tissue front amounts to ~15 s.

Our findings also provide a direct estimate of the average time required for a vesicle to move Mb from the plasma to the interstitial fluid: it appears to be 45–60 s but it should be considered a maximal value, possibly further increased by fixation for which it is clear that we do not have a sharp starting point. The same applies for each of the phases in which we have resolved the transport operation. The figure mentioned (~60 s) can be compared, on the one hand, with calculated values for one effective traverse which range from 5 min (69) to 24 s (1), 3–5 s (84), and 1 s (85), and, on the other hand, with observed values from work with larger probes such as HRP: 5–8 min (2, 4) and ferritin 10 min (1, 4). The observed values increase as expected with increase in probe size, but much more detailed data on the large tracers would be needed for reliable comparison.

So far, the findings reported have been interpreted in terms of Mb transport from the lumen to the pericapillary spaces; we assume that transport in the reverse direction occurs concomitantly and continuously, but it is difficult to detect it in the conditions of our experiments, which rely on a high concentration of Mb in the plasma.

Our counts show that there is considerable variation in the density of vesicle population per cubic micron of endothelium. The frequency increases from time 0 (~800 vesicles/μm^3) to 60 s (~1,050 vesicles/μm^3), but in view of the small volume of our samples and of the large variations in vesicle distribution clearly demonstrated in freeze-cleaved preparations (Simionescu, Simionescu, and Palade, manuscript in preparation) we cannot yet decide whether such variations are significant or not. If confirmed, they may represent an osmotic response to the increase in colloid osmotic pressure in the plasma and interstitial fluid.

INTERCELLULAR JUNCTIONS: During the first 60 s of our experiments, the vast majority of the intercellular junctions of the endothelium appear to be impermeable to Mb within the sensitivity of the procedures we have used. At early time points (0–45 s) the reaction product marks the luminal recesses which lead to the junctions proper but stops at the level of the latter and is not detected in the intercellular spaces past the junctions. At late time points (45–60 s), i.e. at a time when Mb appears to be actively discharged by vesicles on the tissue front of the endothelium, there is reaction product in the intercellular spaces but in concentrations usually lower or equal to those found in the pericapillary areas, or to vesicles discharging in the intercellular spaces on the abluminal side of the junctions. The latter situation can also explain the very rare instances in which the concentration of the reaction product in the intercellular spaces is higher than in the pericapillary regions (Fig. 21 *b*).

Our findings on the permeability of the junctions do not agree with those reported by Karnovsky and his collaborators (2, 3, 9), using HRP as a probe. The disagreement can be explained by differences in specimens (mostly myocardium) and time points examined (intervals longer than 2 min), but also by experimental artifacts caused by excess blood volume (7), or high HRP concentrations which affect capillary permeability (6). There is, however, agreement between our findings with Mb and those reported by Williams and Wissig (4) with HRP in an experimental setup similar to ours.

We can conclude that in our conditions there is no detectable transport of Mb through the intercellular junctions, but we cannot rule out Mb transport at rates below the sensitivity of our procedures, or transport of molecules smaller than Mb along this potential passage. As already mentioned, Karnovsky has recently claimed that cytochrome *c* exists along the intercellular junctions (86).

Freeze-cleaved preparations clearly demonstrate the existence of typical, though simplified tight junctions in the endothelium of muscle capillaries. These junctions are less organized in depth than in other epithelia and form narrow zonulae along which there are suggestions of small focal discontinuities (unpublished observations). In addition, there is increasing physiological evidence on ion and water leaks, presumably through occluding zonules, in other epithelia, e.g., amphibian epithelia (58). All these considerations point out the desirability of extending our approach to probes smaller than Mb and cytochrome *c*, and of postponing any generalization concerning the permeability of the endothelial junctions until more evidence becomes available.

Functional Heterogeneity within the Endothelium

It has been assumed in the past that the peripheral zone of the endothelial cell is the most important, if not the only, functional area as far as transport of macromolecules is concerned. Our Mb experiments show that the frequency of vesicles per cubic micron is the same in this zone and in the thin layer of cytoplasm which surrounds the nucleus; moreover, they indicate that the pattern of vesicular labeling is comparable in the two regions. Since Mb reaches the vesicles on the tissue front of the perinuclear cytoplasm almost as rapidly as in the peripheral zone, although they have to travel around the nucleus, we have to postulate that movement of vesicles is faster in the perikaryon. It is possible that vesicle "diffusion" in the thin cytoplasmic layer surrounding the nucleus is more rapid than in the peripheral zone since it is practically limited to two dimensions. But it is also possible that the distance between the two cell fronts is shortened by short cuts provided by indentations of the nuclear surface. The relatively low transport activity of the organelle region remains unexplained, but seems to be primarily due to slow vesicular uptake and movement. Noteworthy is the limited activity of the parajunctional zone which appears to reflect primarily the low local frequency of plasmalemmal vesicles.

Basement Membrane and Pericapillary Spaces

The basement membrane does not constitute a diffusion barrier for Mb, as expected on account of its coarse porosity: it is known that it does not retain ferritin (1). There is, however, suggestive evidence that Mb may be retained at least temporarily in this layer like in a gel filtration column (80) or that it has some affinity for its glycoproteins or polysaccharides (87). The uneven Mb distribution in the pericapillary spaces may reflect different degrees of restricted diffusion or steric exclusion in the various domains of this highly heterogeneous system (80). The salient finding in connection with these structures and spaces is the very rapid diffusion of Mb once discharged on the tissue front of the endothelium. An exact calculation of its local diffusion rate is not possible since the viscosity of the content of these spaces is unknown and moreover is expected to vary from one domain to another. For a rough estimate, we assumed that the overall viscosity approximates that of the cytoplasm (η = 0.50 P [88]) and we considered an upper and a lower limit to this value each of them removed by one order of magnitude (5.0 and 0.05 P, respectively).[7] On this basis, the diffusion coefficient of Mb in the interstitia is in the range 2.7×10^{-9} cm^2/s to 2.7×10^{-7} cm^2/s. Using the calculated limits of its diffusion coefficient, we estimate that a Mb molecule can move from 6 to 60 μm/min by diffusion in the interstitial matrix. Diffusion at such a rate can explain the rapid decay of initial Mb concentration gradients in the pericapillary spaces, and hence the difficulties we encountered in detecting them. When found, they were usually located in narrow interstitia in which diffusion is expected to be slowed down.

Correlation with the Pore Theory

On the basis of the pore theory and on account of its size (md_{avg} = 33 Å) Mb is expected to reach the interstitial fluid through both pore systems. In muscle capillaries, the plasmalemmal vesicles have been proposed as structural equivalent for the large pore system (1), but the identity and location of the small pores is still in doubt. A slit version located in the intercellular junctions has been repeatedly considered (2, 3, 9) and extensively discussed, so far without agreement as to the exact dimensions (width and length) of the slits. For the length (and depending on the depth of the narrow part of the junctions), values as high as 100% and as low as 3% of the total length of the intercellular junctions have been proposed (68, 70, 91, 92). Our experimental results indicate that Mb can be

[7] D (the diffusion coefficient) has been calculated using the equation: $D = KT/f$, where T is the absolute temperature, f is the frictional coefficient, and K is Boltzmann's constant (89). f has been approximated by applying the Stokes-Einstein equation for large, spherical particles: $f = 6\pi\eta R$, where R is the radius of the particle (in the case of myoglobin 17 Å) and η is the viscosity of the solution (in this case the assumed upper and lower limits). Note that the calculated D of 2.7×10^{-7} cm^2/s coincides with the experimental value reported by Moll (90) for the myoglobin diffusion coefficient in muscle homogenates. The mean displacement of myoglobin by diffusion has been calculated using the Einstein equation for the random walk of a single particle: $\bar{X}^2 = 2Dt$, where $\bar{X}$ is the mean displacement, D is the diffusion coefficient, and t the time in seconds. Thus 6 and 60 μm represent displacements per min calculated using $D = 2.7 \times 10^{-9}$ cm^2/s and $D = 2.7 \times 10^{-7}$ cm^2/s, respectively.

demonstrated in transit through the endothelium in plasmalemmal vesicles, but cannot be detected in the intercellular junctions. The simplest interpretation of these results is that the plasmalemmal vesicles represent both systems. Their correlation with the large pores has already been established, using ferritin as a probe (1). The correlation with the small pore system is more difficult. The plasmalemmal vesicles could function as small pores, provided they incatenate to form continuous channels across the endothelium, and provided these channels be fitted with strictures reducing their lumen to ~90 Å. The first condition has never been proved, but the postulated channels made up of chains of vesicles may be unusually sensitive to fixation. The second condition could be satisfied by the presence of narrow introits (necks) into leading vesicles, strictures at the point of fusion of two vesicles, or diaphragms in between vesicles or at the stoma of discharging vesicles. Such structures have actually been described in visceral and muscle capillaries (1, 93, 94). The large difference in frequency between postulated pores (15–20/μm^2) and found vesicles (~100/μm^2) could be explained by assuming that the formation of connecting channels out of chains of vesicles is an event of relatively low probability.

Our results provide additional supportive evidence for the hypothesis that the vesicles represent both pore systems, but admittedly are not sufficient to prove it. What appears to be needed at present is further evidence bearing on the permeability or impermeability of the intracellular junctions to molecules smaller than Mb, and on the possible existence of chains of vesicles forming connecting channels across the endothelium.

ADDENDUM

After the completion of our work, a paper was published by W. A. Anderson on "The use of exogenous myoglobin as an ultrastructural tracer" (1972, *J. Histochem. Cytochem.* **20**:672). It makes use of the peroxidatic reaction of myoglobin, and it deals mainly with the reabsorption and translocation of this protein by the renal tubule, and includes incidental observations on the fenestrated capillaries of the kidney cortex.

We gratefully acknowledge the excellent technical assistance of Paula Sonnino, Heide Plesken, Elizabeth Szabo, George Davy, and Roland Blischke, and we thank David J. Castle for his help in calculating diffusion coefficients.

This work was supported by United States Public Health Service grant HE 05648.

Received for publication 8 November 1972, and in revised form 19 January 1973.

REFERENCES

1. Bruns, R. R., and G. E. Palade. 1968. Studies on blood capillaries. II. Transport of ferritin molecules across the wall of muscle capillaries. *J. Cell Biol.* **37**:277.
2. Karnovsky, M. J. 1967. The ultrastructural basis of capillary permeability studied with peroxidase as a tracer. *J. Cell Biol.* **35**:213.
3. Cotran, R. S., and M. J. Karnovsky. 1968. Ultrastructural studies on the permeability of the mesothelium to horseradish peroxidase. *J. Cell Biol.* **37**:123.
4. Williams, M. C., and S. L. Wissig. 1971. Permeability of small blood vessels of the diaphragm to horseradish peroxidase (HRPO). A light and electron microscopic study. 11th Annual Meeting of the American Society for Cell Biology, New Orleans.
5. Themann, H., G. Keuker, and V. Westphal. 1971. Elektronenmikroscopische Untersuchungen zur Permeation exogener Peroxidase durch das Endothel der Herzmuskel Kapillaren. *Cytobiologie.* **3**:13.
6. Clementi, F. 1970. Effect of horseradish peroxidase on mice lung capillaries permeability. *J. Histochem. Cytochem.* **18**:266.
7. Schneeberger, E. E., and M. J. Karnovsky. 1971. The influence of intravascular fluid volume on the permeability of newborn and adult mouse lungs to ultrastructural protein tracers. *J. Cell Biol.* **49**:319.
8. Wade, J. B., and V. A. Discala. 1971. The effect of osmotic flow on the distribution of horseradish peroxidase within the intercellular spaces of toad bladder epithelium. *J. Cell Biol.* **51**:553.
9. Karnovsky, M. J. 1970. Morphology of capillaries with special reference to muscle capillaries. *In* Capillary Permeability. Alfred Benzon Symposium II. Ch. Crone and N. A. Lassen, editors. Academic Press, Inc., New York. 341.
10. Dickerson, R. E., T. Takano, D. Eisenberg, O. B. Kallai, L. Samson, A. Cooper, and E. Margoliash. 1971. Ferricytochrome *c*. General features of the horse and bonito proteins at 2.8 Å resolution. *J. Biol. Chem.* **246**:1511.
11. Kendrew, J. C. 1961. The three-dimensional structure of a protein molecule. *Sci. Am.* **205**:96.
12. Kendrew, J. C., H. C. Watson, B. E. Strandberg, R. E. Dickerson, D. C. Phillips, and

V. C. SHORE. 1961. A partial demonstration by X-ray methods, and its correlations with chemical data. *Nature (Lond.)*. **190**:666.

13. URNES, P. J., K. IMAHORI, and P. DOTY. 1961. The optical rotary dispersion of right-handed α-helices in sperm whale myoglobin. *Proc. Natl. Acad. Sci. U.S.A.* **47**:1635.
14. RAY, D. K., and F. R. N. GURD. 1967. Some interrelations between carboxymethylation and heme reactions in sperm whale myoglobin. *J. Biol. Chem.* **242**:2062.
15. ANTONINI, E. 1965. Interrelationship between structure and function in hemoglobin and myoglobin. *Physiol. Rev.* **45**:123.
16. WITTENBERG, J. B. 1970. Myoglobin facilitated oxygen diffusion: role of myoglobin in oxygen entry into muscle. *Physiol. Rev.* **50**:559.
17. ROSSI FANELLI A., E. ANTONINI, and A. CAPUTO. 1964. Hemoglobin and myoglobin. *Adv. Protein Chem.* **19**:73.
18. HARDMAN, K. D., E. H. EYLAR, D. K. RAY, L. J. BANASZAK, and F. R. N. GURD. 1966. Isolation of sperm whale myoglobin by low temperature fractionation with ethanol and metallic ions. *J. Biol. Chem.* **241**:432.
19. HARTZELL, C. R., J. F. CLARK, and F. R. N. GURD. 1968. Hemic acid dissociation in whale, seal and porpoise myoglobins and their alkylated derivatives. *J. Biol. Chem.* **243**:697.
20. CLARK, J. F., and F. R. N. GURD. 1967. Effect of alkylation of sperm whale myoglobin on response to extremes of temperature and pH. *J. Biol. Chem.* **242**:3257.
21. HUGLI, T. E., and F. R. N. GURD. 1970. Carboxymethylation of sperm whale myoglobin in the dissolved state. *J. Biol. Chem.* **245**:1939.
22. FRONTICELLI, C., and E. BUCCI. 1963. Acetone extraction of heme from myoglobin and hemoglobin at acid pH. *Biochim. Biophys. Acta.* **78**:530.
23. GEORGE, P., J. BEETLESTONE, and J. S. GRIFFITH. 1961. Ferrihemoprotein hydroxides: A correlation between magnetic and spectroscopic properties. *In* Hematin Enzymes. J. E. Falk, R. Lemberg, and R. K. Morton, editors. Pergamon Press, Ltd., Oxford. 105.
24. HARRISON, S. C., and E. R. BLOUT. 1965. Reversible confirmational changes of myoglobin and apomyoglobin. *J. Biol. Chem.* **240**:299.
25. BRESLOW, E., S. BEYCHOK, K. D. HARDMAN, and F. R. N. GURD. 1965. Relative conformations of sperm whale myoglobin and apomyoglobin in solution. *J. Biol. Chem.* **240**:304.
26. BANERJEE, R. 1962. Etude thermodynamique de l'association heme-globine. I. Equilibre de dissociation de la metmyoglobine: données thermodynamiques. *Biochim. Biophys. Acta.* **64**:368.
27. AWAD, E. S., and D. A. DERANLEAU. 1968. Thermal denaturation of myoglobin. I. Kinetic resolution of reaction mechanism. *Biochemistry.* **7**:1791.
28. EDMUNDSON, A. B. 1965. Amino-acid sequence of sperm whale myoglobin. *Nature (Lond.)*. **205**:883.
29. TENTORI, L. 1970. Myoglobin, with particular reference to the myoglobin of *Aplysia*. *Biochem. J.* **119**:33P. (Abstr.)
30. DREWS, G. A., and W. K. ENGEL. 1961. An attempt at histochemical localization of myoglobin in skeletal muscle by the benzidine-peroxidase reaction. *J. Histochem. Cytochem.* **9**:206.
31. GOLDFISCHER, S. 1967. The cytochemical localization of myoglobin in striated muscle of man and walrus. *J. Cell Biol.* **34**:398.
32. JAMES, N. T. 1968. Histochemical demonstration of myoglobin in skeletal muscle fibres and muscle spindles. *Nature (Lond.)*. **219**:1174.
33. MORITA, S., R. G. CASSENS, and E. J. BRISKEY. 1969. Localization of myoglobin in striated muscle of the domestic pig: benzidine and $NADH_2$-TR reactions. *Stain Technol.* **44**:283.
34. GOTH, A., and M. KNOOHUIZEN. 1966. Genetically conditioned dextran cofactor in the rat. *Fed. Proc.* **25**:692.
35. SIMIONESCU, N., and G. E. PALADE. 1971. Dextrans and glycogens as particulate tracers for studying capillary permeability. *J. Cell Biol.* **50**:616.
36. COTRAN, R., and M. J. KARNOVSKY. 1968. Resistance of Wistar-Furth rats to the mast cell-damaging effect of horseradish peroxidase. *J. Histochem. Cytochem.* **16**:382.
37. MAJNO, G., and G. E. PALADE. 1961. Studies on inflammation. I. The effect of histamine and serotonin on vascular permeability: an electron microscopic study. *J. Biophys. Biochem. Cytol.* **11**:571.
38. SIMIONESCU, N., M. SIMIONESCU, and G. E. PALADE. 1972. Permeability of intestinal capillaries. Pathway followed by dextrans and glycogens. *J. Cell Biol.* **53**:365.
39. FERNANDEZ, L. A., O. RETTORI, and R. H. MEJIA. 1966. Correlation between body fluid volumes and body weight in the rat. *Am. J. Physiol.* **210**:877.
40. GRAHAM, R. C., and M. J. KARNOVSKY. 1966. The early stage of absorption of injected horseradish peroxidase in the proximal tubule of the mouse kidney. Ultrastructural cytochemistry by a new technique. *J. Histochem. Cytochem.* **14**:291.
41. KARNOVSKY, M. J. 1971. Use of ferrocyanide-reduced osmium tetroxide in electron microscopy. 11th Annual Meeting of the American

Society for Cell Biology, New Orleans. 146. (Abstr.)

42. FARQUHAR, M. G., and G. E. PALADE. 1965. Cell junctions in amphibian skin. *J. Cell Biol.* **26:** 263.
43. MUMAW, V. R., and B. L. MUNGER. 1971. Uranyl-acetate oxalate an en bloc stain as well as a fixative for lipids associated with mitochondria. *Anat. Rec.* **169:**38. (Abstr.)
44. ROCKWELL, A. F., P. NORTON, J. B. CAULFIELD, and S. I. ROTH. 1966. A silicone rubber mold for embedding tissue in epoxy resins. *Sci. Tools.* **13:**9.
45. GEORGE, P., J. BETTLESTONE, and J. S. GRIFFITH. 1961. Ferrihaemoprotein hydroxides: a correlation between magnetic and spectroscopic properties. *In* Hematin Enzymes J. E. Falk, R. Lemberg, and R. K. Morton, editors. Pergamon Press, Ltd., Oxford. 105.
46. HANANIA, G. I. H., A. YEGHIAYAN, and B. F. CAMERON. 1966. Absorption spectra of sperm-whale ferrimyoglobin. *Biochem. J.* **98:**189.
47. MELLEMA, J. E., E. F. J. VAN BRUGGEN, and M. GRUBER. 1967. Uranyl oxalate as a negative stain for electron microscopy of proteins. *Biochim. Biophys. Acta.* **140:**180.
48. MELLEMA, J. E., and E. F. J. VAN BRUGGEN. 1968. An assessment of negative staining in the electron microscopy of low molecular weight proteins. *J. Mol. Biol.* **31:**75.
49. HASCHEMEYER, R. H. 1970. Electron microscopy of enzymes. *Adv. Enzymol. Relat. Areas Mol. Biol.* **33:**71.
50. LEVIN, O. 1963. Electron micrographs of bovine cytochrome *c*. *J. Mol. Biol.* **6:**137.
51. LEVIN, O. 1963. Electron microscopic investigation of the subunit of hemoglobin and the myoglobin molecule. *J. Mol. Biol.* **6:**158.
52. VASSAR, P. S., J. M. HARDS, D. E. BROOKS, B. HAGENBERGER, and G. V. F. SEAMAN. 1972. Physicochemical effects of aldehydes on the human erythrocyte. *J. Cell Biol.* **53:**809.
53. GRANT, R. T. 1964. Direct observation of skeletal muscle blood vessels (rat cremaster). *J. Physiol. (Lond.).* **172:**123.
54. GRANT, R. T., and H. P. WRIGHT. 1968. Further observations on the blood vessels of skeletal muscle (rat cremaster). *J. Anat.* **103:**553.
55. MAJNO, G., V. GILMORE, and M. LEVENTHAL. 1967. A technique for the microscopic study of blood vessels in living striated muscle (cremaster). *Circ. Res.* **21:**823.
56. SMAJE, L., B. W. ZWEIFACH, and M. INTAGLIETTA. 1970. Micropressures and capillary filtration coefficients in single vessels of the cremaster muscle of the rat. *Microvasc. Res.* **2:**96.
57. CARDON, S. Z. 1970. Effect of oxygen on cyclic red blood cell flow in unanesthetized mammalian striated muscle as determined by microscopy. *Microvasc. Res.* **2:**67.
58. DI BONA, D. R. 1972. Passive intercellular pathways in amphibian epithelia. *Nat. New Biol.* **238:**179.
59. JOHNSON, P. C., and F. I. MARCUS. 1970. Regulation of blood flow in skeletal muscle capillaries. VI Conference on Microcirculation, European Society for Microcirculation. Aalborg, S. Karger, Basel. 149.
60. VEGGE, T., F. Ø. WINTHER, and B. R. OLSEN. 1971. Horseradish peroxidase in plasma studied by gel filtration. *Histochemie.* **28:**16.
61. BALINT, A., and Z. NAGY. 1971. Permeability tracers and serum proteins. *Experientia (Basel).* **27:**175.
62. JAVID, J., D. S. FISCHER, and T. H. SPAET. 1959. Inability of haptoglobin to bind myoglobin. *Blood.* **14:**683.
63. LATHEM, W. 1960. The binding of myoglobin by plasma proteins. *J. Exp. Med.* **111:**65.
64. WHEBY, M. S., O'NEILL BARRETT, JR., and W. H. CROSBY. 1960. Serum protein binding of myoglobin, hemoglobin and hematin. *Blood.* **16:**1579.
65. THIESSEN, G., H. THIESSEN, H. J. DOWIDAT, L. LUCIAN, and E. REALE. 1970. Die Diffusion des ^{59}Fe markierten Hämoglobins, ein Artefakt der glutaraldehyde-fixierung. *Histochemie.* **23:**1.
66. GROTTE, G. 1956. Passage of dextran molecules across the blood-lymph barrier. *Acta Chir. Scand. Suppl.* **211:**1.
67. MAYERSON, H. S., C. G. WOLFRAM, H. H. SHIRLEY, JR., and K. WASSERMAN. 1960. Regional differences in capillary permeability. *Am. J. Physiol.* **198:**155.
68. LANDIS, E. M., and J. R. PAPPENHEIMER. 1963. Exchange of substance through the capillary walls. *Handb. Physiol.* **II(2):**961.
69. RENKIN, E. M. 1964. Transport of large molecules across capillary walls. *Physiologist.* **7:**13.
70. PAPPENHEIMER, J. R., E. M. RENKIN, and L. M. BORRERO. 1951. Filtration, diffusion and molecular sieving through peripheral capillary membranes. A contribution to the pore theory of capillary permeability. *Am. J. Physiol.* **167:** 13.
71. PAPPENHEIMER, J. R. 1953. Passage of molecules through capillary walls. *Physiol. Rev.* **33:**387.
72. KUROZUMI, T., Y. INADA, and K. SHIBATA. 1961. Peroxidase activity of hemoproteins. III. Activation of methemoglobin and catalase by formamide and guanidine. *Arch. Biochem. Biophys.* **94:**464.
73. NAKAMURA, Y., T. SAMEJIMA, K. KURIHARA, M. TOHJO, and K. SHIBATA. 1960. Peroxidase

activity of hemoproteins. II. Metmyoglobin and cytochrome *c*. *J. Biochem (Tokyo)*. **48**:862.

74. MARGOLIASH, E., W. M. FITCH, and R. E. DICKERSON. 1971. Molecular expression on evolutional phenomen in the primary and tertiary structures of cytochrome *c*. *In* Biochemical Evolution and the Origin of Life. E. Schoffeniels, editor. North Holland Publishing Co., Amsterdam. 52.
75. KEILIN, D. 1961. Reactions of hemoproteins with hydrogen peroxide and the supposed formation of hydrogen peroxide during the autoxidation of haemoglobin. *Nature (Lond.)*. **191**:769.
76. SELIGMAN, A. M., M. J. KARNOVSKY, H. I. WASSERKRUG, and J. S. HANKER. 1968. Nondroplet ultrastructural demonstration of cytochrome oxidase activity with a polymerizing osmiophilic reagent, diaminobenzidine (DAB). *J. Cell Biol.* **38**:1.
77. NOVIKOFF, A. B., P. M. NOVIKOFF, N. QUINTANA, and C. DAVIS. 1972. Diffusion artifacts in 3,3′-diaminobenzidine cytochemistry. *J. Histochem. Cytochem.* **20**:245.
78. LUFT, J. H. 1965. The ultrastructural basis of capillary permeability. The Inflammatory Process. Academic Press, Inc. New York. 121.
79. SHIRAHAMA, T., and A. S. COHEN. 1972. The role of mucopolysaccharides in vesicle architecture and endothelial transport. An electron microscope study of myocardial blood vessels. *J. Cell. Biol.* **52**:198.
80. LAURENT, T. C. 1970. The structure and function of the intercellular polysaccharides in connective tissue. *In* Capillary Permeability. Alfred Benzon Symposium II. C. Crone and N. A. Lassen, editors. Academic Press Inc., New York. 261.
81. FLITNEY, F. W. 1966. The time course of the fixation of albumin by formaldehyde, glutaraldehyde, acrolein and other higher aldehydes. *J. R. Microsc. Soc.* **85**:353.
82. HOPWOOD, D. 1967. Some aspects of fixation with glutaraldehyde. *J. Anat.* **101**:83.
83. SHEA, ST. M., and M. J. KARNOVSKY. 1969. Vesicular transport across endothelium: simulation of a diffusion model. *J. Theor. Biol.* **24**: 30.
84. CASLEY-SMITH, J. R. 1971. The passage of cytoplasmic vesicles across endothelial and mesothelial cells. *J. Microsc. (Oxf.)*. **93**:167.
85. KARNOVSKY, M. J., and S. M. SHEA. 1970. Transcapillary transport by pinocytosis. *Microvasc. Res.* **2**:353.
86. KARNOVSKY, M. J., and D. F. RICE. 1969. Exogenous cytochrome *c* as an ultrastructural tracer. *J. Histochem. Cytochem.* **17**:751.
87. MORECKI, R., H. M. ZIMMERMAN, and N. Y. BECKER. 1969. Transport of peroxidase by the developing rat choroid plexus. *Acta Neuropathol.* **14**:14.
88. SHEA, ST. M., and M. J. KARNOVSKY. 1966. Brownian motion: a theoretical explanation for the movement of vesicles across the endothelium. *Nature (Lond.)*. **212**:353.
89. TANFORD, C. 1967. Physical Chemistry of Macromolecules. John Wiley and Sons, Inc., New York. 349.
90. MOLL, W. 1968. The diffusion coefficient of myoglobin in muscle homogenate. *Pflügers Arch. Gesamte Physiol. Menschen Tiere.* **299**:247.
91. LASSEN, N. A., and J. TRAP-JENSEN. 1970. Estimation of the fraction of the inter-endothelial slit which must be open in order to account for the observed transcapillary exchange of small hydrophilic molecules in skeletal muscle in man. *In* Capillary Permeability. Alfred Benzon Symposium II. Ch. Crone and N. A. Lassen, editors. Academic Press, Inc., New York. 647.
92. TRAP-JENSEN, J., and N. A. LASSEN. 1970. Capillary permeability for smaller hydrophilic tracers in exercising skeletal muscle in normal man and in patients with long-term diabetes mellitus. *In* Capillary Permeability. Alfred Benzon Symposium II. Ch. Crone and N. A. Lassen, editors. Academic Press, Inc., New York. 135.
93. BRUNS, R. R., and G. E. PALADE. 1968. Studies on blood capillaries. I. General organization of blood capillaries in muscle. *J. Cell Biol.* **37**: 244.
94. PALADE, G. E., and R. R. BRUNS. 1968. Structural modulations of plasmalemmal vesicles. *J. Cell Biol.* **37**:633.